



# UNIVERSITA' DEGLI STUDI DI PADOVA

DIPARTIMENTO DI PEDIATRIA

SCUOLA DI DOTTORATO DI RICERCA  
IN MEDICINA DELLO SVILUPPO E SCIENZE DELLA PROGRAMMAZIONE

Indirizzo Genetica Biochimica e Molecolare

CICLO XXI

**THE BLOOD-BRAIN BARRIER AND SANFILIPPO SYNDROME:  
A MODEL FOR PATHOPHYSIOLOGY STUDIES OF CNS  
IN LYSOSOMAL STORAGE DISEASES**

**Direttore della Scuola:** Ch.mo Prof. Giuseppe Basso

**Supervisore:** Ch.mo Dott. Maurizio Scarpa

**Dottorando:** Eva Zaccariotto



# INDEX

<b>RIASSUNTO</b>	<b>3</b>
<b>ABSTRACT</b>	<b>5</b>
<b>INTRODUCTION</b>	<b>7</b>
Lysosomal storage diseases and lysosome	7
Mucopolysaccharidoses	9
Sanfilippo syndrome or mucopolysaccharidosis type III	13
• <u>Mucopolysaccharidosis type IIIA</u>	14
• <u>Mucopolysaccharidosis type IIIB</u>	15
Therapies	16
Blood-brain barrier	18
Animal models for MPSIIIA and IIIB	24
<b>OBJECTIVES</b>	<b>27</b>
<b>MATERIALS AND METHODS</b>	<b>29</b>
Mice	29
<i>In situ</i> brain perfusion	29
Perfusion fluid	30
Perfusion setup	30
Scintillation counting	31
Calculation	32
Statistics	33
Capillary depletion	33
Saturation curve	33
Electron microscopical studies	34
Intraperitoneal injections	34
<b>RESULTS</b>	<b>35</b>
Perfusion parameters	35

Brain regions	35
Cerebral blood flow	36
Vascular space	38
Excitatory amino acids	39
Electron microscopical analyses	41
Sanfilippo type IIIA mice	42
Sanfilippo type IIIB mice	48
Intraperitoneal injections	51
<b>DISCUSSION</b>	<b>53</b>
<b>REFERENCES</b>	<b>59</b>

## RIASSUNTO

Le patologie d'accumulo lisosomiale (LSD) rappresentano un grosso ed eterogeneo gruppo di malattie genetiche che derivano da difetti in diversi aspetti della biologia lisosomiale. Queste patologie interessano più comunemente i bambini, e per la maggior parte determinano coinvolgimento neurologico che, quando presente, non è trattabile.

Tutti gli animali con un sistema nervoso centrale (SNC) ben sviluppato hanno una barriera emato-encefalica (BEE) che isola ampiamente il cervello dalle alterazioni nella composizione del flusso del sangue e dai continui cambiamenti che avvengono in generale in questi fluidi corporei. Questa barriera impedisce anche la somministrazione globale al SNC di molte sostanze terapeutiche. Diversi studi condotti in modelli murini delle malattie d'accumulo lisosomiale, come le patologie di Batten, Sandhoff e GM1 gangliosidosi, hanno inoltre suggerito che la BEE possa essere danneggiata come parte integrante del processo patologico. Lo scopo del presente progetto è stato quello di determinare se avvenissero simili cambiamenti nella BEE nella sindrome di Sanfilippo. La tecnica della perfusione cerebrale *in situ* è il sistema di elezione per questo studio in quanto per le molecole analizzate non è necessario considerare gli effetti dovuti ad eventuali legami con le proteine plasmatiche, metabolismo e altre interazioni all'interno del corpo. Inoltre, offre una sensibilità superiore rispetto ad altri metodi basati su tracciante e può essere usata per quantificare precisamente il trasporto di soluti attraverso la BEE. Abbiamo apportato una nuova modifica alla tecnica originale di Takasato e Smith (1984) che assicura che tutte le regioni del cervello del topo siano perfuse piuttosto che solo la zona di una singola carotide. Questo è importante poiché nelle LSD tutte le regioni cerebrali sono coinvolte e il *circulus arteriosus cerebri* presenta differenti gradi di completezza in diversi ceppi murini (Ward *et al.* 1990). Quindi il metodo permette che la funzione della BEE sia valutata in tutte le regioni, e può essere applicato per comparare animali modificati geneticamente di diversi background genetici. Diversi parametri, come il flusso della perfusione cerebrale, il volume vascolare del cervello, e il trasporto carrier-mediato degli amminoacidi acido glutammico e glicina, sono stati investigati per determinare se il metodo della perfusione cerebrale *in situ* possa essere applicato al topo senza disturbare l'integrità fisica e funzionale della BEE. Sono stati anche condotti studi con nitrato di lantano, e analizzati al microscopio elettronico, per valutare se le giunzioni occludenti subissero aperture durante il corso della perfusione.

Una volta che la tecnica della perfusione cerebrale *in situ* è stata provata come strumento reale per la valutazione della penetrazione di traccianti attraverso la BEE, questo metodo è stato

applicato per determinare se ci fossero cambiamenti nella BEE in modelli murini di due forme della sindrome di Sanfilippo (MPS IIIA e MPS IIIB) in confronto ai loro rispettivi ceppi murini di controllo. [<sup>14</sup>C]-saccarosio e [<sup>3</sup>H]-inulina sono stati impiegati per valutare il volume vascolare, ma normalmente non penetrano la membrana, a meno che non sia difettiva. [<sup>14</sup>C]-diazepam è stato utilizzato come marker del flusso sanguigno cerebrale; e [<sup>3</sup>H]-glicina, [<sup>3</sup>H]-acido glutammico e [<sup>3</sup>H]-tirosina come sostanze carrier-mediate a bassa penetrazione cerebrale. Questi sono amminoacidi neuro-eccitatori che possono causare danni al cervello se la loro entrata nel cervello è aumentata. Dati iniziali per la sindrome di Sanfilippo dalla tecnica della perfusione cerebrale *in situ*, sebbene necessitino di essere confermati e approfonditi, hanno dimostrato la tipica eterogeneità clinica dei pazienti di Sanfilippo ed evidenziano chiaramente che avvengono alcuni cambiamenti nella BEE.

Anche la permeabilità di [<sup>3</sup>H]-N-butil-deossinojirimicina (NB-DNJ, miglustat, Zavesca®) alla BEE è stata valutata poichè è attualmente impiegata nella terapia di riduzione del substrato (SRT), si ritiene che penetri la BEE e teoricamente potrebbe essere usata per trattare l'accumulo secondario nella sindrome di Sanfilippo. Da iniezioni intraperitoneali di [<sup>3</sup>H]- NB-DNJ e valutazione della costante d'influsso unidirezionale  $K_{in}$  per intervalli di tempo fino a 60 minuti, un lento ma progressivo assorbimento di questa piccola molecola è stato dimostrato.

Una comprensione maggiore della BEE e della sua funzione, sia in salute sia in malattia, è assolutamente e criticamente necessaria per lo sviluppo di farmaci nuovi e migliori che possano riparare la BEE e in più siano anche in grado di attraversare la BEE allo scopo di trattare manifestazioni precoci della sindrome di Sanfilippo nel SNC. Questi studi produrranno informazioni che aiuteranno la somministrazione di farmaci al SNC in generale e aumenteranno ulteriormente la possibilità di trattare un ampio numero di patologie neurodegenerative.

## ABSTRACT

The lysosomal storage diseases (LSDs) are a large and heterogeneous group of disorders resulting from defects in various aspects of lysosomal function. They commonly afflict infants and young children and mostly involve pathology of the brain which is currently untreatable when it's present. All animals with a well developed central nervous system (CNS) have a blood-brain barrier (BBB) that largely isolates the brain from alterations in the composition of the blood stream and the continuous changes that take place in these general body fluids. This BBB also impedes the global CNS delivery of many therapeutic materials. Some studies in mouse models of lysosomal storage diseases, such as Batten and Sandhoff diseases and GM1 gangliosidosis, have also suggested that the BBB may be damaged as an integral part of the disease process. The aim of the present project was to determine whether similar changes to the BBB occur in Sanfilippo Syndrome. The *in situ* brain perfusion technique is the elective system for this study as it is not necessary to consider the effects of plasma binding, metabolism and other interactions within the body. Furthermore, it offers a superior sensitivity over other tracer based methods and can be used to precisely quantify the transport of solutes across the BBB. We developed a novel modification of the original technique of Takasato and Smith (1984) which ensures that all regions of the mouse brain are perfused rather than just the territory of a single carotid artery. This is important as in LSDs all brain regions are affected and in different mouse strains the *circulus arteriosus cerebri* exhibits different degrees of completeness (Ward *et al.* 1990). Thus the method allows full regional BBB function to be assessed, and the method can be applied to a comparison of genetically modified animals on differing genetic backgrounds. Several parameters, such as cerebral perfusion flow, brain vascular volume, and carrier-mediated transport of excitatory amino acids glutamic acid and glycine, were then investigated to determine whether the *in situ* brain perfusion method may be applied to the mouse without disturbance to the physical or functional integrity of the BBB. Electron microscopy studies with lanthanum nitrate were also performed to assess whether the tight junctions became leaky during the course of perfusion.

Once the *in situ* brain perfusion technique was established as a real tool for assessing the penetrance of tracers across the BBB, this method was applied to determine if there were changes to the BBB in mouse models of two of the Sanfilippo Syndrome diseases (MPS IIIA and MPS IIIB) compared with their respective control strains of mouse. [<sup>14</sup>C]-sucrose and [<sup>3</sup>H]-inulin were used to assess vascular volume, but do not normally penetrate the BBB, unless it is defective. [<sup>14</sup>C]-diazepam was used as a marker of cerebral blood flow; and [<sup>3</sup>H]-glycine, [<sup>3</sup>H]-

glutamic acid and [<sup>3</sup>H]-tyrosine as carrier-mediated substances with low brain penetrance. These are neuro-excitatory amino acids which can cause brain damage if their entry into brain is increased. Initial findings in Sanfilippo syndrome from *in situ* brain perfusion technique, though they need to be confirmed and examined more fully, showed the typical clinical heterogeneity of Sanfilippo patients and clearly highlight that some changes occurred in the BBB.

Also the BBB permeability of [<sup>3</sup>H]- *N*-butyl-deoxynojirimycin (NB-DNJ, miglustat, Zavesca®) was assessed as it is currently employed for substrate-reduction therapy (SRT), is believed to penetrate the BBB and theoretically could be used to treat secondary storage in Sanfilippo Syndrome. From intraperitoneal injections of [<sup>3</sup>H]- NB-DNJ and evaluation of the unidirectional influx constant  $K_{in}$  for time intervals up to 60 minutes, a slow but progressive brain uptake of this small molecule was demonstrated.

An improved understanding of the BBB and its function, both in health and disease, is absolutely and critically necessary for development of successful new and improved drugs that may repair the BBB and in addition are also capable of crossing the normal BBB in order to further treat early CNS manifestations of Sanfilippo Syndrome. These studies will produce information which will aid drug targeting in general to the CNS and will further advance the possibility of treating a wide range of neurodegenerative diseases.

# INTRODUCTION

## Lysosomal storage diseases and lysosome

The Lysosomal Storage Diseases (LSDs) are a heterogeneous group of approximately 50 inherited metabolic disorders, which most commonly affect infants and young children, classified as rare diseases with an overall occurrence of 1:7000 live births (Meikle *et al*, 1999). They, thus, represent globally a very significant health and economic burden and in some isolated geographical regions and societies the occurrence of specific lysosomal storage disorders can be relatively much higher. LSDs arise from mutations affecting the activity of either lysosomal hydrolases, transferases involved in transport across the lysosomal membrane, or in ancillary proteins which affect post-translational processing of enzyme or trafficking of enzyme into and out of the lysosome. A lysosomal defect leads to accumulation of undegraded material causing cell and organ dysfunction. The characterization of the specific metabolic and genetic defects that underlie these diseases have markedly increased our understanding of lysosomal biology. Initially discovered by Christian de Duve (1964), lysosomes are now known to contain more than 50 acid hydrolases that can digest most of the intracellular and extracellular macromolecules. Lysosomal enzymes are synthesized in the rough endoplasmic reticulum and then transferred to the *cis*-Golgi, where they acquire mannose-6-phosphate (M6P) residues. This recognition marker is specific to lysosomal hydrolases and allows them to be sorted from other proteins. The phosphorylated enzymes bind to Mannose-6-Phosphatate (M6P) receptors that are located in the membranes of the vesicles that bud from the *trans*-Golgi network. These transport vesicles fuse with other acidic vesicles (such as late endosomes and lysosomes), leading to the dissociation of the lysosomal enzymes from the M6P receptors. The receptors then recycle back to the Golgi. Macromolecules to be catabolized or processed are delivered to the lysosome either by engulfment or by fusion of digestive vacuoles with the lysosomes. Catabolism takes place within the lumen of the lysosomes at an acidic pH, which is maintained by a specific proton pump in the lysosomal membrane (Fig. 1) (Desnick and Schuchman, 2002).

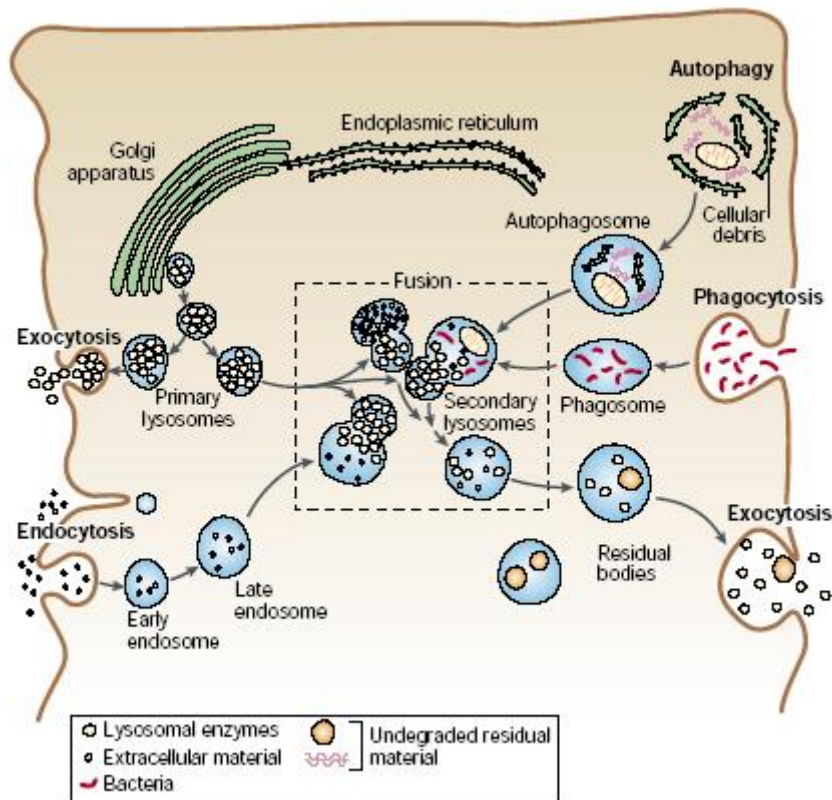


**FIG 1.** The endosomal-lysosomal apparatus (Desnick and Schuchman, 2002).

Many steps are necessary for synthesis and processing of lysosomal enzymes; therefore it is not surprising that a dysfunction of this system may result from manifold mechanisms. Indeed, the number of recognized LSDs is increasing as new disorders are characterized biochemically and genetically.

Most LSDs are inherited in an autosomal recessive manner, with the exception of Hunter syndrome or mucopolysaccharidosis type II (MPS II), which shows X-linked recessive inheritance; Danon disease, which is X-linked dominant; and Fabry disease, which, with a high proportion of affected females, should not be described as X-linked recessive.

The lysosomal storage disorders can be classified according to the molecular enzymic genetic defect and to the substrate that is accumulating in the affected cells; for example, lipid storage disorders, mucopolysaccharidoses and glycoproteinoses. Each involved enzyme or protein may be affected by mutations which will alter enzymic or other activity to differing extents. Mutations may be silent and not affect enzyme function or they may affect enzyme activity mildly, moderately, severely or totally abolish catalytic activity. Thus within each recognised lysosomal storage disorder there may be multiple forms of the disease with either a severe or an attenuated course.

Although the precise genetic defect and the resulting change in amino acid sequence, structure and activity of the affected and damaged protein is now well documented for these diseases, the link between the defect, accumulation of storage product and pathology is poorly understood. The storage product that accumulates is usually the substrate for the affected enzyme, however, other storage products may also accumulate. In fact, a single degradation pathway is rarely involved and an affected degradation pathway may then overload other parallel pathways, or cause accumulation of substrate further down the degradation pathway as some catalysed steps may be more rate limited than others. Some tissues place a greater demand on these degradation pathways than others and are often the most severely affected, liver, spleen, heart and bone are peripheral tissues commonly involved, resulting in massive hepatosplenomegaly, heart and valve defects and cardiac failure, skeletal deformities, short stature and dysostosis multiplex. All of these are coupled to other LSD specific features such as coarse faces, eye and ear impairments, respiratory insufficiency is often the major cause of death in early adolescence. Up to 70% of the lysosomal storage disorders involve substrate accumulation in brain tissue with resulting neuropathology and CNS cell death (Platt *et al*, 2004). Again neuronopathic progression may be rapid and severe with death in early years or more prolonged and attenuated with a number of decades of survival.

## **Mucopolysaccharidoses**

More than 10 diseases are related to the degradation of mucopolysaccharides (or glycosaminoglycans, GAG) heparan-, dermatan-, keratan- and chondroitin-sulphate, with consequent accumulation of harmful amounts of these big molecules singly or in combination, and progressive cellular damage. As there are various types of glycosaminoglycans that differ in sugar composition and, as these are distributed in tissues throughout the human body, the mucopolysaccharidoses manifest as multi-organ diseases.

GAGs are long unbranched polysaccharide chains composed of repeating disaccharide units; one of the two sugar residues is always an amino sugar, as N-acetylgalactosamine (GalNAc) or N-acetylglucosamine (GlcNAc), the second sugar is usually an uronic acid, as glucuronic acid or iduronic acid.

Because there are sulphate or carboxyl groups on most of their sugar residues, GAGs are highly negatively charged and therefore attract  $\text{Na}^+$  cations, that are osmotically active. For this reason GAGs are strongly hydrophilic and form porous hydrated gels, thus their chains fill most of the

extracellular space, providing mechanical support to tissues while still allowing the rapid diffusion of water-soluble molecules and the migrations of cells.

Glycosaminoglycans degradation proceeds stepwise from nonreducing end by the action of glycosidases and sulfatases (Fig. 2).

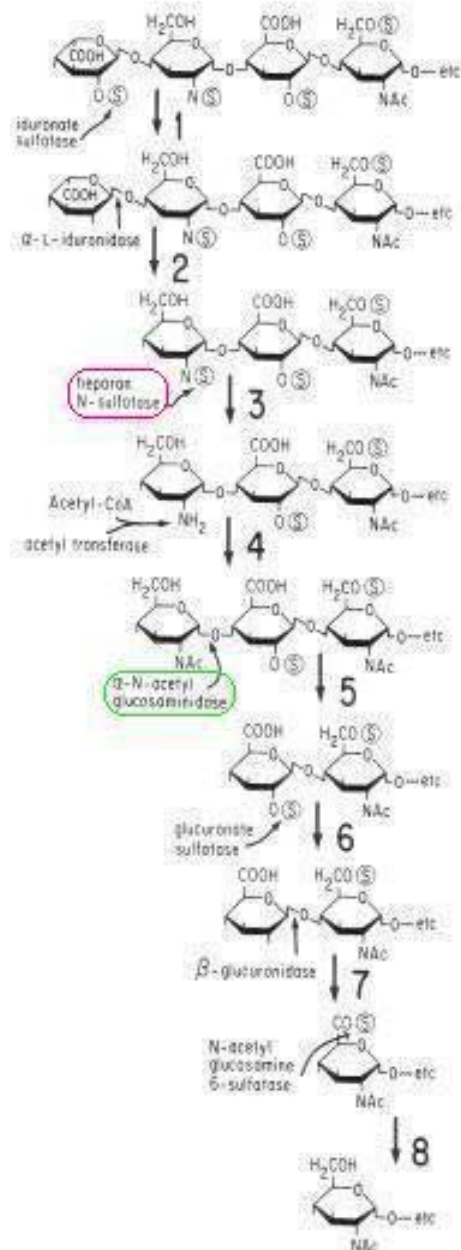


**FIG 2.** Stepwise degradation of heparan sulphate (Neufeld and Muenzer, 2001). In particular, deficient enzyme in MPS IIIA is highlighted in purple and deficient enzyme in MPS IIIB is highlighted in green.

GAGs are covalently linked to a core protein. The complex, as such, is called a proteoglycan. Proteoglycans are produced and secreted by fibroblasts, chondrocytes and osteocytes, forming loose connective tissue, cartilage and bone, respectively. In these tissues, the proteoglycans form a large molecular complex with hyaluronic acid and collagen, filling the spaces between the

cells. Hyaluronic acid, dermatan-sulphate, chondroitin-sulphate, heparin, heparan-sulphate and keratan-sulphate are physiologically relevant, and although each glycosaminoglycan has a specific disaccharide unit (Fig. 3), a remarkable heterogeneity exists within each class of GAGs (Alberts *et al*, 1996 Zanichelli Ed.).

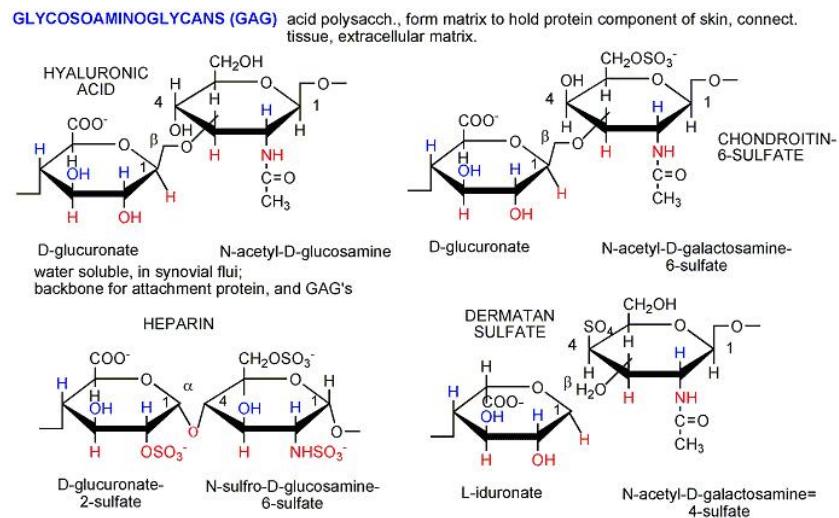


**FIG 3.** Disaccharide units composing the glycosaminoglycans (Lodish *et al*, 2000).

Indeed each mucopolysaccharidoses (MPS) represents a broad continuum of severity and range of manifestations. The MPS disorders have a chronic, progressive course, although the age of the onset of symptoms and severity of clinical disease can vary markedly. Most of the disorders are characterized by multisystem involvement, abnormal facies, organomegaly, and dysostosis multiplex. Clinical presentation, severity of symptoms, and central nervous system involvement can vary widely both within and between the seven major types, distinguished by the specific enzyme deficiency, the major clinical features, or both (Table 1). Note that designations V and VIII are no longer used and that only one patient has been described with type IX.

Number*	Eponym	Enzyme deficiency	Glycosaminoglycan stored
MPS I (severe)	Hurler syndrome	$\alpha$ -L-iduronidase	Dermatan sulfate, heparan sulfate
MPS I (attenuated)	Scheie syndrome	$\alpha$ -L-iduronidase	Dermatan sulfate, heparan sulfate
MPS I (attenuated)	Hurler-Scheie syndrome	$\alpha$ -L-iduronidase	Dermatan sulfate, heparan sulfate
MPS II (severe)	Hunter (severe) syndrome	Iduronate sulfatase	Dermatan sulfate, heparan sulfate
MPS II (attenuated)	Hunter (mild) syndrome	Iduronate sulfatase	Dermatan sulfate, heparan sulfate
MPS IIIA	Sanfilippo A syndrome	Heparan N-sulfatase	Heparan sulfate
MPS IIIB	Sanfilippo B syndrome	$\alpha$ -N-acetyl-glucosaminidase	Heparan sulfate
MPS IIIC	Sanfilippo C syndrome	Acetyl CoA: $\alpha$ -glucosaminide acetyltransferase	Heparan sulfate
MPS IIID	Sanfilippo D syndrome	N-acetylglucosamine 6-sulfatase	Heparan sulfate
MPS IVA	Morquio syndrome, type A	Galactose-6-sulfatase	Keratan sulfate, chondroitin 6-sulfate
MPS IVB	Morquio syndrome, type B	$\beta$ -galactosidase	Keratan sulfate
MPS VI	Maroteaux-Lamy syndrome	N-acetylgalactosamine 4-sulfatase (arylsulfatase B)	Dermatan sulfate
MPS VII	Sly syndrome	$\beta$ -glucuronidase	Dermatan sulfate, heparan sulfate chondroitin 4-,6-sulfates
MPS IX		Hyaluronidase	Hyaluronan

**TABLE 1.** Biochemical classification of the mucopolysaccharide disorders (Muenzer, 2004).

All MPS disorders with the exception of MPS III have distinct somatic manifestations. Patients with MPS III have only subtle somatic manifestations but marked central nervous system involvement, resulting in severe mental retardation, hyperactivity, and behavioural problems. Patients with the severe forms of MPS I, MPS II, and MPS VII also have progressive mental retardation.

In addition to glycosaminoglycans, several gangliosides (GM2, GM3, and GD3) accumulate in the brains of MPS patients with mental retardation (Constantopoulos *et al*, 1978 and 1980). This accumulation has been puzzling, since their catabolism does not require the enzymes of glycosaminoglycan degradation. However, the activity of several additional lysosomal enzymes is reduced in the MPS, probably as a result of inhibition by accumulated glycosaminoglycans.

Mucopolysaccharidoses often initially present subtly. Most affected children with an MPS disorder appear normal at birth and only later in infancy or childhood begin to display signs or symptoms. Because most of the patients excrete increased amounts of mucopolysaccharides in the urine, this analysis together with enzyme assays are the elective systems for diagnosis. Any patient diagnosed with an MPS disorder based on clinical findings does not have a confirmed diagnosis until the suspected enzyme deficiency is documented. All diagnostic testing should be overseen by a clinician who has expertise in lysosomal storage disorders, because the assays are complex and results can be difficult to interpret. Detection of these disorders permits genetic counselling for the parents, with the option of prenatal diagnosis in subsequent pregnancies. The effectiveness of potential therapies, for disorders such as mucopolysaccharidoses that involve central nervous system and bone pathologies, would rely heavily on the early diagnosis and

treatment of the disorder, before the onset of irreversible pathology. In the absence of a family history, the only practical way to identify affected individuals presymptomatically is through a newborn screening program. Newborn screening for selected LSDs is under development (Chamoles *et al*, 2004; Meikle *et al*, 2004).

### **Sanfilippo syndrome or mucopolysaccharidosis type III**

Mucopolysaccharidosis type III is the most common form of MPS. Prevalence range approximately from 1:70000 to 1:100000 births. Patients with Sanfilippo syndrome make up a biochemically diverse but clinically similar group of four recognizes types. The deficient enzymes for the Sanfilippo subtypes are heparan N-sulfatase (type A);  $\alpha$ -N-acetylglucosaminidase (type B); acetyl CoA: $\alpha$ -glucosaminide acetyltransferase (type C); and N-acetyl glucosamine 6-sulfatase (type D). The four enzymes are required for the degradation of heparan sulphate.

Phenotypic variation exists in MPS III patients but to a lesser degree than in other MPS, possibly because a very mild form of MPS III would be difficult to recognize. MPS III histopathology reveals vacuolation in neurons, glia, and perivascular cells. The accumulation of abnormal heparan sulphate species likely affects signalling by members of the fibroblast growth factor family, which have important functions in the development and plasticity of neural cells. Heparan sulphate storage presumably induces the accumulation of ganglioside GM2 in lysosomes as well as ganglioside GM3 and cholesterol accumulation in late endosomes, lysosomes and other cell membranes. Heparan sulphate and GM2/GM3 ganglioside accumulation affect calcium homeostasis, axonal transport, neurite growth, synaptogenesis, loss of plasticity and cell survival (Li *et al*, 2002). The different subtypes are characterized by severe central nervous system degeneration, but only mild somatic disease. The usual clinical findings are of a severe progressive neurologic disease. Onset of clinical features usually occurs between 2 and 6 years in a child who previously appeared normal. Patients with Sanfilippo syndrome loose acquired skills such as speech, normal gait, and toilet training. Later, aggressive behaviour, hyperactivity and sleep disturbances occur. The hair is coarse, often blond, and hirsutism may be present. Bone changes are mild. MPS III patients are of normal height, sometimes have seizures and become tetrapastic in the first or second decade of their life; they usually die of respiratory complications, heart failure or infection.

Each of the MPS III types is inherited as an autosomal recessive disorder. Geographic distribution reported for European populations is uneven, with the A subtype prevalent in Northern Europe, the B subtype most common in Southern Europe, MPS IIIC less frequent than subtypes A and B and only few patients with MPS IIID described (Neufeld and Muenzer, 1995). Type A is claimed to be the most severe of the four Sanfilippo subtypes with earlier onset of symptoms and more rapid progression whereas type B shows a wider clinical heterogeneity with mild and severe cases reported.

### **Mucopolysaccharidosis type IIIA**

A deficiency in the lysosomal hydrolase heparan N-sulphatase (HNS) is responsible for storage and excretion of excessive amounts of heparan sulphate leading to the pathogenesis of Sanfilippo A (mucopolysaccharidosis type IIIA) syndrome (Fig. 2). This enzyme is involved in the hydrolysis of the sulphamate bond in 2-sulphamino-glucosamine residues present in heparan sulphate and heparin.

HNS has been purified from human liver, kidney and placenta (Freeman and Hopwood, 1986). The estimated molecular mass of the mature protein is 56 kDa and of the native protein 100 to 125 kDa. The mature protein consists of 502 amino acids and the optimal pH for the enzyme activity is 6.8. The isolation, sequence and expression of cDNA clones encoding the enzyme have been determined (Scott *et al*, 1995). The predicted molecular mass of the enzymically active sulphamidase corresponds to the HNS purified from human liver. There are five potential N-glycosylation sites, with N41 shown to be functional from amino acid sequencing. Residues Cys70 and Arg74 of the sulphamidase consensus sulphatase signature (SSCSPSRASLLTG) are conserved and might be involved in the catalytic mechanism of sulphatases. The other conserved signature region amino acids 115 to 124 (GVRTGIIGKK) is also present. In addition, Asp31 is conserved among the sulphatase protein sequences and may also be a catalytic residue.

The heparan N-sulphatase gene has been localised to chromosome 17q25.3 and contains a total of 8 exons that span approximately 11 kb. It has been found that the intron boundaries were flanked by highly conserved consensus splicing signals. The HNS gene produces three major mRNA transcripts (3.1, 4.3, and 7.1 kb), with the 3.1 kb transcript being the predominant mRNA species in most tissues. No consensus polyadenylation site was found in the 3'-untranslated region of the cDNA, although four copies of a 57 bp tandem repeat have been identified in the 3' UTR. These repeats were not found to be polymorphic and have been proposed as consensus (Karageorgos *et al*, 1996).

In MPS IIIA there is a large genetic heterogeneity, together with recurrent mutations: R245H seems to be of Western European origin (Weber *et al*, 1997) whereas S66W has a reasonably high incidence in Italian MPS IIIA patients (Di Natale *et al*, 1998). Not surprisingly, mutation frequencies of British and Australasian patients are similar, with the exception of S66W higher frequency in Australian patients, consistent with the migration pattern of Southern Europeans to Australia over the past few generations. Reported results include several single base pair mutations and a few small deletions/insertions. These mutations concern amino acids in conserved positions in consensus sequences (R74C, G122R) or close to the consensus (S66W), presumably destroying the structure and function of the active site; in other conserved amino acids (Y40N, L146P), changing the protein structure; in restriction sites (R245H); in nonconservative amino acids (R377C, A44T) and C-terminal (R377H). Interpretation of the clinical phenotype is very difficult. For instance, although sulphatases share very little homology in their C-terminal domains, some positions result in severe phenotypes suggesting that they should be conservative and important for enzyme function; furthermore, homoallelic patients for the conservative exchange S66W develop severe or intermediate phenotypes, suggesting that other genetic or epigenetic factors could modulate patient phenotype.

### **Mucopolysaccharidosis type IIIB**

The basic defect in Sanfilippo B disease (mucopolysaccharidosis III B) is a profound deficiency in activity of  $\alpha$ -N-acetylglucosaminidase (NAG) (Fig. 2). In a concerted action with the other three MPS III deficient enzymes, NAG accomplishes the removal of the variably substituted  $\alpha$ -linked glucosamine residues from heparan sulphate.

The glycosidase has been purified from several tissues and species with a reported molecular mass for precursor and intermediate or mature forms approximately ranging from 86 kDa to 77 and 73 kDa.

The full-length NAG cDNA has been determined and codes for the 743 amino acids of the enzyme and 101 bp 5'-non-translated sequence as well as 245 bp 3'-non-translated region including a polyadenylation-signal and a potential polyA-tail. There are seven potential N-glycosylation site and at least one is glycosylated (Weber *et al*, 1996).

The  $\alpha$ -N-acetylglucosaminidase gene, localised to chromosome 17q21.1, is interrupted by five introns and is 8.2 kb long from translation start to polyadenylation site. Molecular characterisation of MPS IIIB patients has resulted in the identification of several mutations in the NAG gene. The base substitutions causing replacement of arginine by a termination codon or by histidine, R297X, R626X, R643H, and R674H, all occur at CpG sites, known to be mutagenic

hotspots. The 10-nt deletion starting with nucleotide 503 occurs at a direct repeat of a tetranucleotide, GGAG, and may be the result of slipped mispairing during DNA replication (Zhao *et al*, 1996). The high degree of molecular heterogeneity reflects the clinical variability observed with MPS IIIB. Certain mutations, such as R297X, show a higher prevalence. R297X is associated with a severe Sanfilippo phenotype when inherited in a homozygous fashion and this is consistent with the highly elevated levels of <sup>35</sup>S-labelled GAG storage in homozygous R297X/R297X skin fibroblasts. The presence of an attenuated Sanfilippo phenotype in a F48L/R297X compound heterozygous patient suggests that the F48L allele is associated with an attenuated phenotype and this has been proved by a residual level of F48L-NAG activity and subsequent partial turnover of GAG (Yogalingam *et al*, 2000).

## **Therapies**

A number of therapies exist for treating the lysosomal storage disorders ranging from enzyme replacement therapy (ERT), substrate reduction therapies (SRT) or enzyme enhancement therapy (EET). In the past, no specific therapy was available for the affected patients, and management consisted solely of supportive care and treatment of complications.

The concept of enzyme replacement therapy for lysosomal storage diseases was first proposed by de Duve in 1964. Thereafter, the discovery that intracellular and secreted lysosomal glycoproteins are targeted to the lysosome by the mannose-6-phosphate (M6P)-receptor-mediated pathway and, importantly, only 1-5% of normal cellular activity was required to correct the metabolic defects in enzyme-deficient cells, indicated the feasibility of ERT. Recombinant DNA techniques for manufacturing highly purified therapeutic enzymes, the development of eukaryotic expression systems to produce large quantities of recombinant enzyme and the use of gene-targeting techniques to generate knock-out mouse models for preclinical studies, have led to the practical application of ERT. In ERT an active version of the defected lysosomal enzyme is infused intravenously. The recombinant enzyme is taken up by cells and transported to the lysosome where it catalyses the missing step in the degradation pathway, thus reducing storage and ameliorating the resulting signs and symptoms. It is important to note that the pH optimum of these lysosomal hydrolases is so acid that they only have significant enzyme activity within the lysosomal compartment.

More recently, ERT has been developed for the MPSs, but although systemic manifestations improve with ERT, treatment has not had an effect on CNS disease. It has been shown that the

lowest concentrations of M6P-receptors are in muscle and brain (Wenk *et al*, 1991). The level of the BBB transport system for acid hydrolases and the high molecular weight of these enzymes thus render any paracellular or transcellular diffusion of these proteins across the BBB almost non-existent.

Because of the inherent difficulties in delivering enzymes across the BBB, approaches utilizing small molecules that have the ability to cross into brain parenchyma are also being developed. Substrate reduction therapy involves small molecules that inhibit early stages in biosynthesis of the substrates that accumulate in these diseases. By inhibiting the activity of these early enzymes, accumulation of storage product is reduced. Enzyme enhancement therapy is based on small molecules which induce the correct conformational folding in the nascent enzyme within the endoplasmic reticulum and thus acting as a chaperone and ensuring proper intracellular trafficking and delivery to the lysosomal compartment. Indeed, some missense mutations and small in-frame deletions may lead to a misfolded protein without significantly affecting the active site. Many of the SRTs and related molecules also are able to function as chaperones. In summary, all these small molecules may be therapeutically useful for LSDs caused by mutant but yet catalytically active enzymes. SRT and EET are not currently available for mucopolysaccharidoses.

In spite of the new therapeutic options, allogenic bone marrow transplantation (BMT), hematopoietic stem cell therapy (HSCT), and, more recently, umbilical cord blood transplantation still play a role in the therapeutic intervention for many LSDs that have significant brain involvement, although therapeutic efficacy has been variable. If some of these transplanted cells are

progenitors for circulating mononuclear cells capable of transmigrating across the BBB and transforming into microglia with a capacity for synthesising and releasing lysosomal hydrolases within the brain this then becomes a strategy for initiating enzyme synthesis behind the BBB. As in ERT, once certain symptoms have developed they become largely irreversible, thus the earlier in life transplantation is performed the better. Transplantation, however, is associated with significant risks, including the development of graft-versus-host disease, graft rejection, early death from infection, and regimen associated toxicity. It is interesting to note that transplantation is more successful at reversing neuropathology in some LSDs, as MPS I, compared to others, including MPS III, which have not responded well to such treatment. A possible explanation might be that the brain, in common with other tissues, has a greater dependence on some specific lysosomal hydrolytic pathways than others and some may be more critically rate-limiting for the overall efficiency of a certain pathway. The slow transmigration of transplant- derived cells

across the Blood Brain Barrier (BBB) might be sufficient to supply enzymic catalytic demand in one LSD but not in another (Begley *et al*, 2008).

LSDs are excellent candidates for gene therapy because they represent generally well-characterized single gene disorders, are not subject to complex regulation mechanisms, and need low level of enzyme activity for clinical efficacy. For *in vivo* gene therapy several viral vectors were used as vehicles for transduction in a depot organ. The beneficial effect of gene transduction into the liver or other tissues is restricted to peripheral organs, as the enzyme that is secreted into the circulation will not cross the blood–brain barrier, therefore, vector delivery systems have been developed for direct *in vivo* gene transfer into the CNS. For *ex vivo* gene therapy stem cells of the patient are transfected with the gene and thereafter returned to the body. Although gene therapy studies performed in animal models are rather promising, many important issues regarding safety and efficacy of this therapeutic strategy need to be addressed before clinical trials can be initiated. To achieve high enzyme activity a high level of transgene expression by hematopoietic stem cells might be required and the integration of a large amount of vectors increases the risk of integrated-dependent adverse events.

Currently, the most successful approaches to deliver therapeutic compounds unable to traverse the BBB to the brain are based on direct intrathecal injection, intraventricular administration, and BBB disruption by chemical agents. These invasive approaches can however only be used for unique administrations, but not for long term therapy as required for the treatment of neurodegenerative disorders and effort needs to be directed at designing, active enzyme preparations that can be transcytosed across the BBB possibly exploiting its natural transport mechanisms.

## **Blood-brain barrier**

All organisms with a well developed central nervous system (CNS) have a blood-brain barrier (BBB). In all mammals the BBB is created by the endothelial cells forming the capillaries of the brain and spinal cord microvasculature and has a total surface area of 12 to 18 m<sup>2</sup> in human, thus it is by far the most important interface for blood-brain exchange. In addition, the BBB is created by the epithelium of the choroid plexuses together with the epithelial ependyma enclosing the circumventricular organs (CVOs), and the avascular arachnoid membrane underlying the dura which completely encloses the entire CNS.

The BBB has essentially a neuroprotective role. It exists to create the special fluid environment that the brain requires to function and it protects the brain from potentially damaging chemicals in the blood. The nerve cells, which form the thinking and functional part of the brain, require an absolutely constant chemical environment for their work. They communicate with each other via chemical neurotransmitters that transfer information from one nerve cell to another. Some of these excitatory neurotransmitters are, for example, the naturally occurring amino acids glycine and glutamic acid which are present in blood in much greater concentration than in the fluids bathing the brain. If it were not for the BBB these excitatory neurotransmitters would rapidly enter the brain and cause inappropriate nerve cell activation and nervous activity and brain damage. A number of large molecular weight proteins that are normally present in blood in significant concentrations are albumin, prothrombin and fibrinogen. These proteins are intensely irritating to brain cells and stimulate glial cell division and glial scarring as well as cause neuroexcitation. These naturally occurring blood proteins are again kept in very low concentration in the brain fluids by the BBB.

Also circulating in blood are a large number of xenobiotics, neurotoxic molecules which are acquired from the environment or the diet. Many of these molecules, because of their chemical properties, would otherwise be able to enter the brain and accelerate nerve cell death causing pre-senile dementia.

A crucial aspect of BBB function is the creation of tight junctions, promoted by a close associations with the end-feet of glial cells, between endothelial cells of the brain capillaries, and the epithelial cells of the choroid plexuses and CVOs, and arachnoid membrane. The BBB is also closely associated with pericytes, microglia, and nerve endings (Fig.4). The tight junctions effectively seal the paracellular aqueous diffusional pathways, preventing the free diffusion of macromolecules, polar solutes, and ions from blood to brain. This impediment results in the high *in vivo* electrical resistance of the BBB.

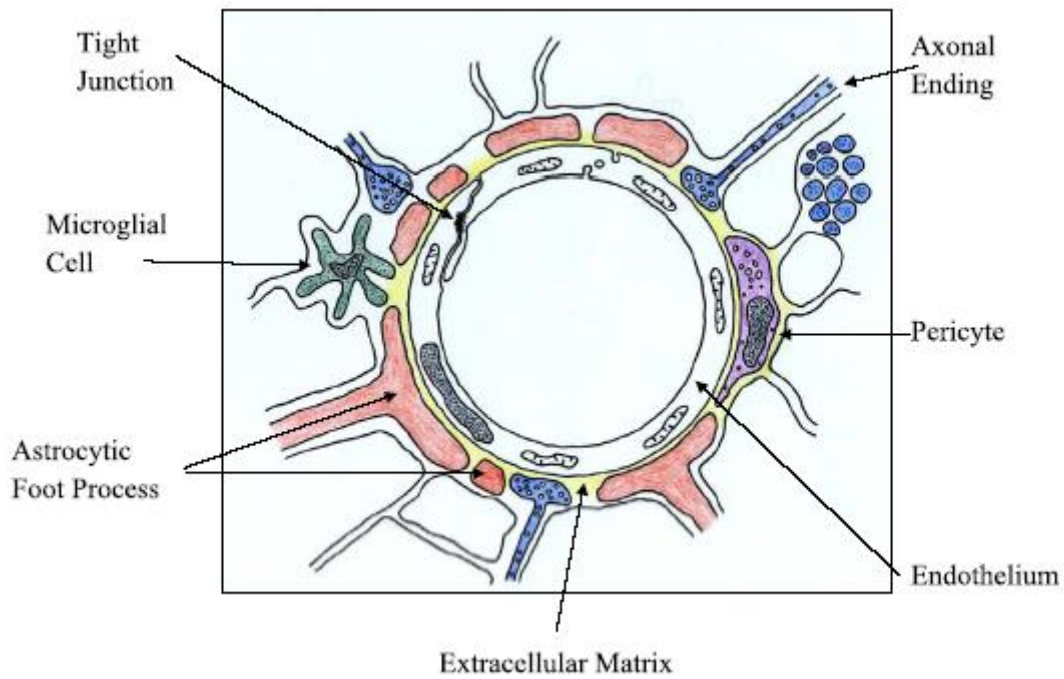


**FIG 4.** Schematic diagram of the neurovascular unit/cell association forming the BBB (Begley, 2004).

Clearly the BBB cannot completely isolate the brain from the blood as there are a large number of specific molecules that the brain requires in order to live and function. Specific transport systems therefore are expressed in the BBB to ensure an adequate supply of these substances (Fig. 5).

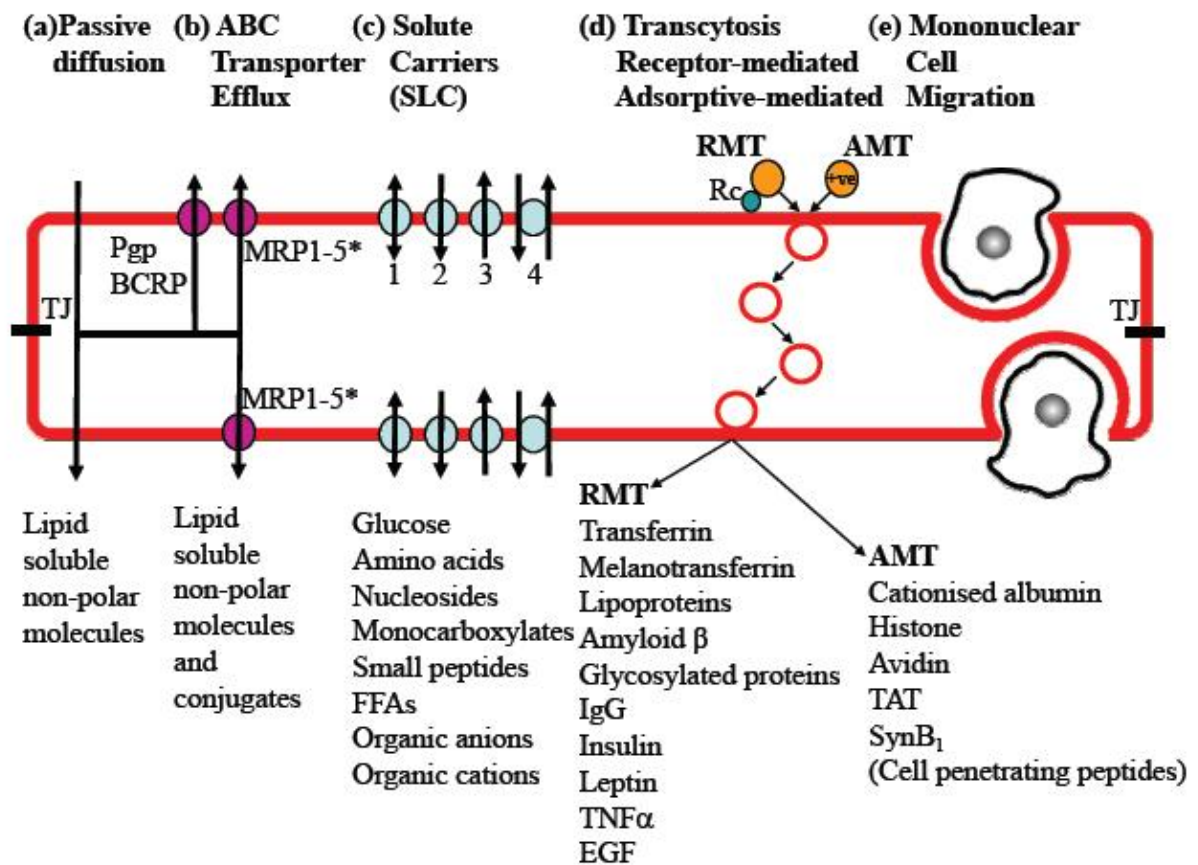


FIG 5. Routes across the BBB (Begley, 2007).

A wide range of lipid-soluble molecules can diffuse through the BBB and enter the brain passively. Factors that restrict the entry of compounds into the CNS are high polar surface area greater than  $80 \text{ \AA}^2$ , a tendency to form more than six hydrogen bonds, the presence of a number of rotatable bonds in the molecule and a molecular weight in excess of 450 Da.

Many essential polar nutrients such as glucose and amino acids that are required for metabolism are transported by specific solute carriers. Some of these transport proteins are inserted into both membranes of the endothelial cells, and others are polarized in their expression and inserted into either the luminal or the abluminal membrane only, to prevent free movement from one side of the endothelium to the other, thus strictly preserving the polarity of the barrier.

The major role of the ABC transporters is to function as active efflux pumps consuming ATP and transporting a diverse range of lipid-soluble chemical compounds out of the CNS and brain capillary endothelium, thus removing from the brain potentially neurotoxic endogenous or xenobiotics molecules and carrying out a vital neuroprotective and detoxifying function.

Specific and some nonspecific transcytotic mechanisms exist to transport a variety of large molecules and complexes across the BBB. These vesicular mechanisms involve either receptor-mediated transcytosis (RMT) or absorptive-mediated transcytosis (AMT). In RMT, the binding

of macromolecular ligands to specific receptors on the cell surface triggers an endocytic event carrying the macromolecules across the endothelium; in AMT, an excess positive charge on the molecule, which renders it highly cationic, appears, in this case, to induce endocytosis and subsequent transcytosis.

In the normal BBB, mononuclear cells appear to penetrate by a process of diapedesis directly through the cytoplasm of the endothelial cells, closing the luminal cell membrane over themselves before opening the abluminal membrane, thus without transitorily opening the barrier.

As the enzymes used in current replacement therapy (ERT) for lysosomal storage diseases do not cross the BBB, alternative methods for achieving transcytosis into the CNS need to be explored. Terminating the enzyme with a ligand for one of the RMT mechanisms for large molecules may provide a mechanism. Suitable candidates might be the Apo receptors transporting apolipoprotein across the BBB, the receptor for advanced glycosylation end-products (RAGE) and the heparin binding epidermal growth factor-like receptor. Using a monoclonal antibody to the transferrin receptor avoids competition with endogenous circulating transferrin and interaction of antibody with the receptor appears to initiate RMT (Bickel *et al*, 1994).  $\beta$ -galactosidase enzyme has been successfully delivered to the mouse brain by directly coupling it to an 8D3 monoclonal antibody to the transferrin receptor (Zhang *et al*, 2005). Cationizing lysosomal hydrolases or attaching a cationic cell penetrating peptide may also offer an opportunity. Cell penetrating peptide have been used to carry also large protein across the BBB (Schwarze *et al*, 1999).

Liposome and nanoparticles are large constructs and can theoretically carry significant amounts of adsorbed or encapsulated enzyme, drug, or other content across the BBB.

The BBB develops during fetal life and is well formed by birth, especially to proteins and macromolecules. Some studies raise the interesting suggestion that mechanisms that might carry lysosomal enzymes across the BBB may be present in early life and then become down-regulated as the individual ages (Urayama *et al*, 2004). What probably happens during the ontogenesis of the BBB is that the variety of receptors, useful for its formation, expressed on the luminal surface of the endothelial cells that are able to induce a transcytotic event become markedly reduced and therefore transcytosis through the BBB is consequentially very selective. To what extent this occurs in the human neonate is unknown. A down-regulated mechanism may be capable of reactivation and of transporting ERT into the CNS.

*N*-butyl-deoxynojirimycin (NB-DNJ) is a small moderately lipophilic molecule, used for substrate reduction therapy, which apparently crosses the blood-brain barrier. Its lipophilicity

may give it sufficient passive permeability to enter the CNS by purely diffusive mechanisms, but it also contains a sugar residue, which may be reactive with a BBB transporter. The mechanism by which NB-DNJ enters cells and crosses the BBB needs to be fully elucidated so that the necessary physico-chemical properties for BBB penetration can be preserved in second generation substrate-depleting drugs.

Some studies have suggested that in some lysosomal storage diseases the BBB itself may be altered. Possible mechanisms might result from accumulation of storage product in the endothelial cells themselves or as a secondary event following microglial activation and associated inflammatory cascades. A study by Jeyakumar *et al.* (2003) with mouse models of Sandhoff disease and GM1 gangliosidosis have shown an increased extravasation of Evans blue-albumin and endogenous immunoglobulin G in both of these mouse models. This permeabilization of the BBB could be linked to inflammatory processes occurring in the CNS. Microglial activation has been noted in mouse models of Mucopolysaccharidosis I and IIIB (Ohmi *et al.*, 2003). Extravasation of immunoglobulin has also been observed in a mouse model of Juvenile Batten disease (Lim *et al.*, 2007).

Thus it seems clear that the BBB may be damaged and altered in a number of lysosomal storage diseases and consequently become more permeable to many blood-borne solutes. If the BBB integrity is compromised low molecular weight neuroexcitatory amino acids glutamic acid and glycine will tend to move down their concentration gradient into brain, as well as significant plasma proteins normally excluded from brain by the BBB. The excitatory amino acid transporters (EAATs), re-uptake mechanisms expressed in the cell membranes of neurones and glial cells and in the abluminal membrane of the BBB which combine to keep the brain extracellular levels of excitatory amino acids low, and the cysteine protease inhibitor cystatin C, one of the few proteins in CSF found in higher concentration than in plasma which inactivate a limited and transient extravasation of prothrombin and other serine proteases, may be then overwhelmed by a significant pathological increase in BBB permeability.

Damage to the BBB may contribute significantly to CNS damage, in addition to the neuropathology resulting from the accumulation of storage products, and the relationship between the two processes needs to be clarified so that novel BBB permeant preparations can be designed in order to restore barrier function and treat LSD.

## **Animal models for MPS IIIA and IIIB**

For many lysosomal storage diseases naturally occurring animal models have been described, such as cats, dogs, cattle and mice, and these models have been used for pathogenetic and therapeutic studies. Many of these animal models, however, are not well suited for research due to the size of the animals and their long reproductive cycle; furthermore, of course not all diseases have been found in animals. Thus, naturally occurring and knockout mice with LSDs have proven extremely valuable.

MPS IIIA has been described as naturally occurring in dogs (Fischer *et al*, 1998 and Jolly *et al*, 2000) and in a murine model (Bhaumik *et al*, 1999) which has been employed in this project. The spontaneous mouse mutant is specifically deficient in sulphamidase activity, like patients with MPS IIIA, and accumulates heparan sulphate that has glucosamine-N-sulphate nonreducing ends, as expected if sulphamidase is inactive, as well as gangliosides, as suggested from detection of abnormal accumulation of GM2 ganglioside in neurons of cerebral cortex. Other lysosomal hydrolases are for the most part increased in activity, a common characteristic of many lysosomal storage diseases (Neufeld and Muenzer, 1995). The fact that residual activity was evident in tissue extract from affected mice suggested, and later it was confirmed, that the mouse mutation is likely to be a point mutation that reduces sulphamidase activity, similar to the mutations observed in humans with MPS IIIA. In the MPS IIIA mice, brain section revealed neurons with distended lysosomes filled with membranous and floccular materials with some having a classical zebra body morphology. Storage materials were also present in lysosomes of cells of many other tissues. Affected mice usually die at 7-10 months of age exhibiting a distended bladder and hepatosplenomegaly.

In recent years spontaneous animal forms of Sanfilippo syndrome type IIIB have been discovered in emu (Aronivich *et al*, 2001) and dog (Ellinwood *et al*, 2003). Li *et al*. (1999) developed a murine model of MPS IIIB, employed in this project, disrupting exon 6 of Naglu, the homologous mouse gene encoding  $\alpha$ -N-acetylglucosaminidase. These and further studies (Heldermon *et al*, 2007) revealed that Naglu  $-/-$  mice show the chronic and progressive course that is characteristic of human lysosomal storage diseases. Biochemical, pathological, and behavioural changes become more pronounced with time. Although the mice were healthy and fertile while young, the effects of the disease became outwardly obvious after 6 months. Naglu  $-/-$  mice could survive for 8–12 months. They were totally deficient in  $\alpha$ -N-acetylglucosaminidase and had massive accumulation of heparan sulphate in liver and kidney as well as secondary changes in activity of several other lysosomal enzymes in liver and brain and elevation of

gangliosides GM2 and GM3 in brain. Vacuolation was seen in many cells, including macrophages, epithelial cells, and neurons, and became more prominent with age. Neuronal cell loss with concomitant astrocyte activation was also demonstrated. The MPS IIIB mouse model had behavioural deficits and progressive deterioration of balance, vision, and hearing similar to human MPS IIIB.

These mouse models are an important source of knowledge in order to understand the complex chain of events between the underlying genetic defect and the phenotypic abnormalities as well as to test treatment strategies.



## OBJECTIVES

Studies into the blood-brain barrier (BBB) are extremely important to understand its function under physiological conditions as well as during a diseased state, where the barrier itself may be defective and contribute towards pathology of the disease (Banks 1999). In order to develop successful new and improved drugs that may repair the BBB and, in addition, are also capable of crossing the normal BBB to treat the CNS it is absolutely necessary to improve our understanding of the BBB and its function, both in health and disease. The aim of the present PhD project was to determine whether changes to the BBB occur in Sanfilippo Syndrome due to the storage of GAG in the endothelial cells composing the MPSIII BBB, a phenomenon that has been demonstrated in other lysosomal storage diseases including Batten (Lim *et al*, 2007), GM1 gangliosidosis and Sandhoff disease (Jeyakumar *et al*, 2003). As the genetics causing LSDs is known, animal models of these diseases exist that allow the study of the loss and recovery of neuro-plasticity upon restoration or compensation of the genetic defect. These animal models are ideal for deciphering the common mechanisms and features of neurodegeneration in general, to identify biomarkers for loss of brain plasticity in neurodegenerative diseases in general and LSDs in particular, and to assess new therapeutic restorative approaches. Two mouse models of MPS IIIA and MPS IIIB, which develop pathology and symptoms and are very similar to the human syndromes, were employed. The *in situ* brain perfusion technique was adapted for use in the mouse to explore the integrity and function of the BBB in these and control mice as they age. The *in situ* technique is advantageous over other systems as it is not necessary to consider the effects of plasma binding, metabolism and other interactions within the body. Once the extent of BBB involvement and pathology in the mouse models MPS III is established we can then evaluate its possible contribution to the progress of the disease. New treatment strategies can then be devised to help repair the BBB and also treat the disease. The development of methods allowing transit of BBB by exploitation of the natural transport pathways will represent a major breakthrough for the long-term therapy of neurodegenerative diseases in general.



## MATERIALS AND METHODS

### Mice

Male C57BL/6 mice of a young adult age (6-9 weeks), weighing 17-20 g, were employed initially to assess the *in situ* brain perfusion technique.

Afterwards the technique was used in mouse models of two of the Sanfilippo syndrome diseases (MPS IIIA and MPS IIIB) and their respective control strains of mouse, at 4-6 and 8-10 months of age.

### *In situ* brain perfusion

Animals were heparinised (Multipharm) and anaesthetised with intraperitoneal injections of ketamine (75 mg/kg, Pharmacia) and medetomidine (1 mg/kg, Pfizer). An incision was made exposing the chest cavity and jugulars. The salivary glands were weighted down with artery clips so the jugulars were easily accessible prior to perfusion. The thorax was held back and ligations loosely made around the descending aorta and the heart. The heart was held taut with a small artery clip and a small incision was made in the left ventricle. A fine cannula of outside diameter 0.96 mm and internal diameter 0.58 mm was threaded through the base of the left ventricle and inserted into the root of the aorta before it was withdrawn slightly and ligatured in place. The descending aorta was then tied off at the level of the base of the left ventricle and both jugulars were severed before commencement of the perfusion. A perfusion flow rate of 10ml/min was required to achieve 1.24 ml/g/min in the mouse brain, which is comparable to physiological blood flow rates measured in the intact animal by other methods (Maeda, 2000; Majid, 2000). The perfusion was terminated by decapitation of the animal. The brain was removed immediately and dissected into different regions before being processed in preparation for scintillation counting.

## Perfusion fluid

Mice were perfused with a physiological saline solution containing (mM): 117 NaCl, 4.7 KCl, 24.8 NaHCO<sub>3</sub>, 1.2 KH<sub>2</sub>PO<sub>4</sub>·3H<sub>2</sub>O, 2.5 CaCl<sub>2</sub>·2H<sub>2</sub>O, 0.8 MgSO<sub>4</sub>·7H<sub>2</sub>O, 10 HEPES, and 10 D-glucose. Prior to perfusion D-glucose was added and the saline solution was gassed with 95% O<sub>2</sub>, 5% CO<sub>2</sub> (vol/vol) for 5 minutes. The saline solution was then adjusted to pH 7.4, passed through a syringe filter (0.45 µm diameter) and warmed to 37° C. For penetration studies, <sup>14</sup>C and <sup>3</sup>H labelled substances were introduced into the perfusate at concentrations of 0.1 µCi/ml. [<sup>14</sup>C]-sucrose (Amersham) and [<sup>3</sup>H]-inulin (Perkin-Elmer) were used to assess vascular volume; [<sup>14</sup>C]-diazepam (Amersham) as a marker of cerebral blood flow; [<sup>3</sup>H]-glutamic acid (Perkin-Elmer), [<sup>3</sup>H]-glycine and [<sup>3</sup>H]-tyrosine (Amersham) as carrier-mediated substances with low brain penetrance. Also the BBB permeability of [<sup>3</sup>H]- *N*-butyl-deoxynojirimycin (NB-DNJ, miglustat, Zavesca®) (Amersham) was assessed as it is currently employed for substrate-reduction therapy of glycosphingolipid storage in Type 1 Gaucher Disease (and theoretically could be used to treat secondary CNS storage in Sanfilippo Syndrome) and is currently believed to penetrate the BBB.

## Perfusion setup

The *in-situ* brain perfusion setup is shown below in Fig. 6. The perfusate was infused into the animal by a slow-drive syringe pump (Harvard), which was kept at a constant 37° C in a heating unit and delivered at a rate of 10 ml/min. All tubing was Portex fine bore polythene, as this is inert to a range of chemicals and is lightweight and flexible. The perfusion pressure was continuously monitored via a pressure transducer that was calibrated to a manometer and displayed on a computer using Chart V4.0 software (AD instruments).

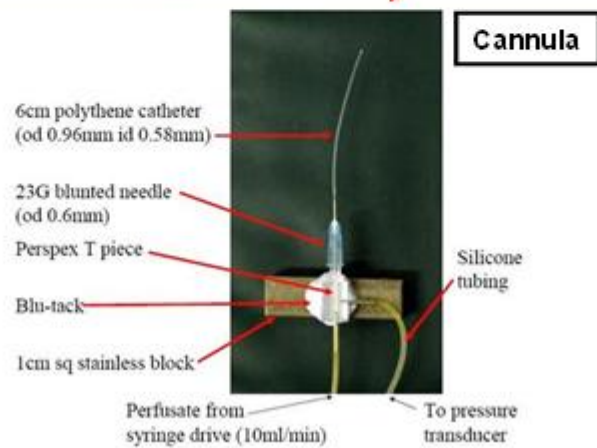
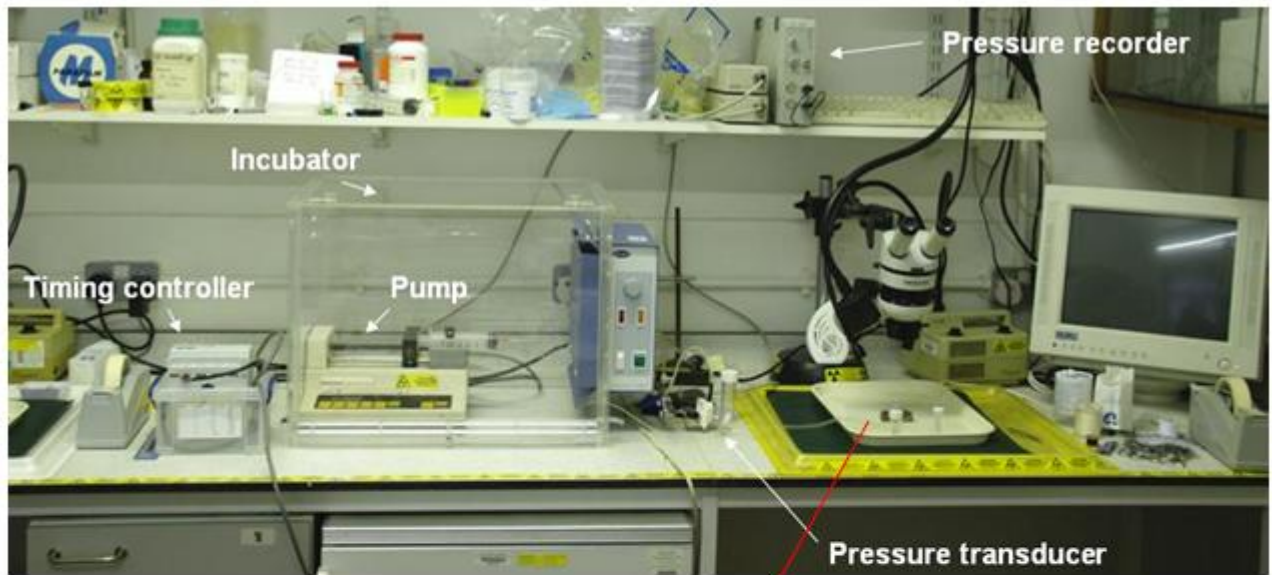
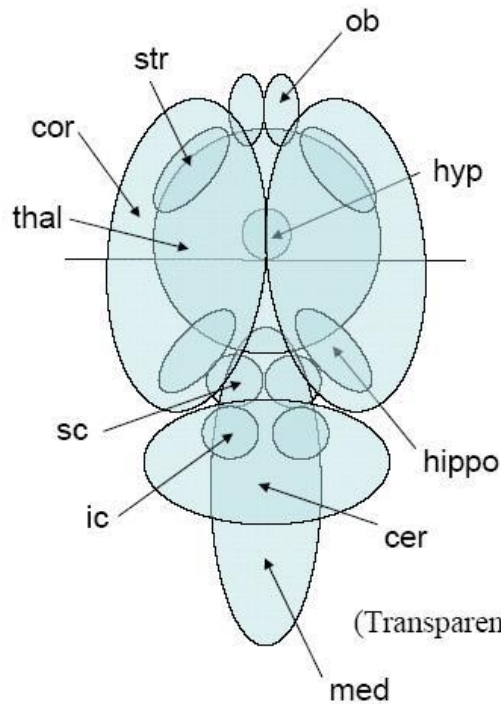


**FIG 6.** Perfusion apparatus.

## Scintillation counting

The whole brain was divided into the following regions: olfactory bulbs (OB), anterior cortex with striatum (left and right hemispheres, ACL and ACR), posterior cortex with hippocampus (left and right hemispheres, PCL and PCR), midbrain with thalamus and hypothalamus (MID), medulla (MED), and cerebellum (CER) (Fig. 7). Brain samples were placed into pre-weighed vial inserts and solubilized overnight in 0.5 ml Solvable (Perkin-Elmer). Samples were then treated with 4 ml scintillation fluid, Ultima Gold (Perkin-Elmer), and counted on a TRI-CARB beta scintillation spectrophotometer (Perkin-Elmer) using a pre-calibrated quench curve programme.



### Samples (8)

1. Olfactory bulbs
2. R Anterior cortex inc. striatum
3. L Anterior cortex inc. striatum
4. R Posterior cortex inc. hippocampus
5. L Posterior cortex inc. hippocampus
6. Cerebellum
7. Medulla (brainstem)
8. Midbrain (inc. sup. and inf. colliculi, thalamus and hypothalamus)

**FIG 7.** Brain regions taken as samples.

### Calculations

The uptake of radiolabelled tracers into the brain was expressed as a volume of distribution ( $V_d$ ).  $V_d$  is defined as the ratio of the radioactivity per unit weight of brain ( $C_{br}$ ) and radioactivity per unit volume of perfusate ( $C_{pf}$ ):

$$V_d = C_{br}/C_{pf}$$

, where  $V_d$  is expressed as ml/g of brain.

The unidirectional transfer constant of a tracer across the BBB was expressed by  $K_{in}$  and was graphically determined from brain uptake data for different lengths of perfusion. This is summarised by the following equation:

$$K_{in} = C_{br}/C_{pf}(T)$$

, where  $T$  is the duration of perfusion, and  $K_{in}$  is the unidirectional transfer constant for a single time point and is expressed as ml/g/min.

## Statistics

Values are displayed as mean  $\pm$  S.E.M, unless otherwise stated. The statistical significance of differences between quantitative data was assessed using a Mann-Whitney U test (GraphPad Prism V 3.02), with statistical significance considered at  $P \leq 0.05$ . \*\* were assigned at  $P \leq 0.01$ , \*\*\* at  $P \leq 0.001$ , and NS when not significant.

## Capillary depletion

Following a 2 minute perfusion with [ $^{14}\text{C}$ ]-sucrose into the perfusate, animals were killed by decapitation and the brain removed for capillary depletion using a dextran density centrifugation as previously described by Triguero (1990). The brain was homogenised at 4° C (10 strokes) in 2 times the volume of a physiological buffer at pH 7.4 containing: 10 mM HEPES, 141 mM NaCl, 4 nM KCl, 2.8 mM  $\text{CaCl}_2$ , 1 mM  $\text{MgSO}_4$ , 1 mM  $\text{NaH}_2\text{PO}_4$ , and 10 mM D-glucose. Dextran solution was then added to a final concentration of 19% and homogenised for a further 5 strokes. An aliquot of homogenate was taken and the remainder centrifuged at 5400 g for 15 minutes at 4° C. The supernatant and pellet were carefully separated and radioactivity measured as described above.

Results were calculated as  $V_d$  for the homogenate (whole brain), pellet (capillary enriched fraction) and supernatant (parenchyma) as described above.

## Saturation curve

To determine the saturability of carrier-mediated transporters for the amino acids with low brain penetrance glutamic acid and glycine, increasing concentrations of unlabelled amino acid were added to the perfusion fluid containing the corresponding labelled amino acid.

Parameter estimates of  $V_{max}$  and  $K_m$  were obtained by nonlinear regression analysis (GraphPad Prism V 3.02).

## Electron microscopical studies

The *in situ* brain perfusion technique was used also to fix the brain of wild type C57BL/6 mice, and HNS mice and their control strains of mouse, of a young adult age (6-9 weeks), in order to conduct electron microscopical analyses.

Animals were perfused at a flow rate of 10 ml/min with 50 ml of a fixation buffer at pH 7.4 containing: paraformaldehyde 16%, glutaraldehyde 50%, cacodylate buffer 0.4 M, lidocaine 2%, heparin 25000 IU/ml and lanthanum 10%.

After the perfusion the brains were kept in a post-fixation buffer containing paraformaldehyde 16%, glutaraldehyde 50% and cacodylate buffer 0.4 M for at least 4 hours, and then dissected in slices containing the following regions in preparation for electron microscopical analyses: olfactory bulbs, cortex, striatum, hippocampus, cerebellum and hindbrain.

## Intraperitoneal injections

[<sup>3</sup>H]- NB-DNJ was also used to assess brain uptake after intraperitoneal injection in 6 week old C57BL/6 mice. Anaesthetised animals were injected with 5 μCi of Zavesca® ip and blood sample was obtained from the carotid artery after intervals of 5, 10, 20, 30, 40, 50 and 60 minutes. Brain was removed, dissected and processed as usual, blood sample was centrifuged for 4 minutes at 3000 rpm at 4° C and obtained plasma processed in preparation for scintillation counting.

The unidirectional transfer constant  $K_{in}$  of Zavesca® across the BBB was calculated from the following equation:

$$K_{in} = C_{br} / \int_0^T C_{pl}(t) dt$$

, where  $C_{pl}$  is the radioactivity per unit volume of plasma and the function at the denominator is called AUC (Area Under plasma concentration time Curve). For multiple time point regression  $C_{br}/C_{pl}$  was plotted against AUC.

## RESULTS

### Perfusion parameters

The perfusion pressure within an animal was calculated by subtracting the back pressure within the system from the overall pressure on the trace (Fig. 8). This pressure remained between 40-80 mmHg, which did not exceed the physiological blood pressure for an adult mouse (Janssen and Smith, 2002).

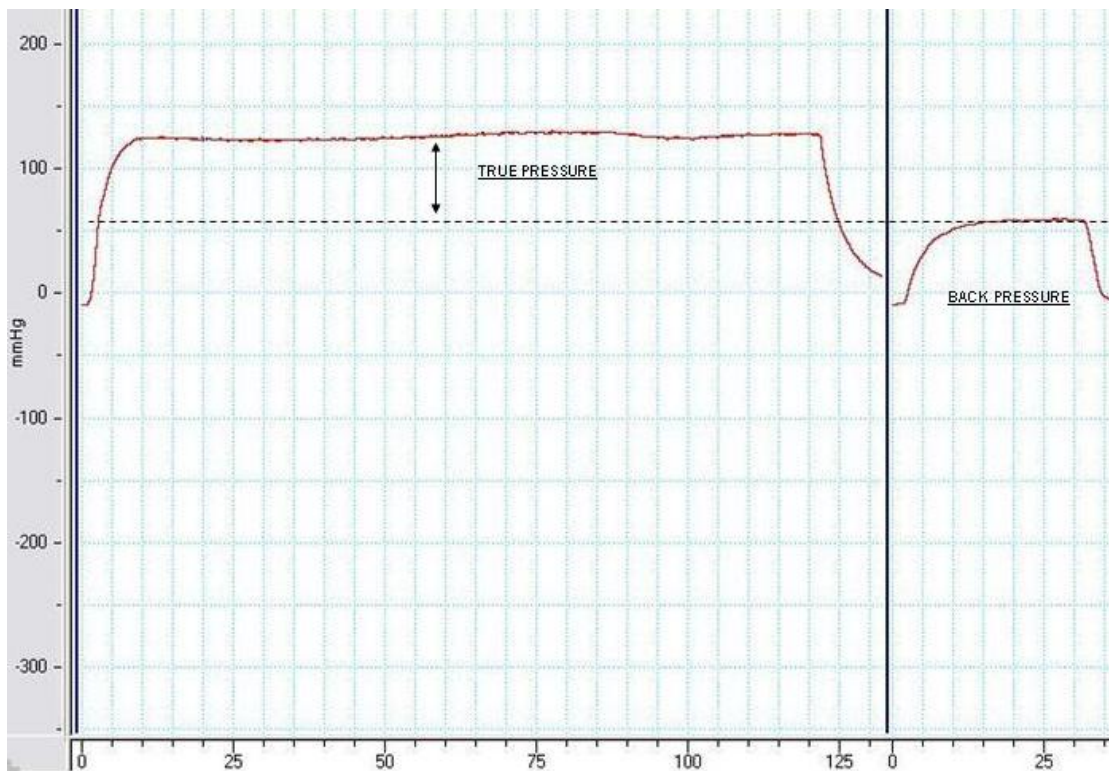


**FIG 8.** Pressure trace after a perfusion. The first trace represents the overall pressure in 2 minutes of perfusion (time in second on the figure), and the second one is the back pressure within the system.

### Brain regions

Overall brain weight ( $413.27 \text{ mg} \pm 5.45$ ) and the weight of individual brain regions that were selected for this study (olfactory bulb  $16.87 \text{ mg} \pm 0.99$ , anterior cortex left  $57.03 \text{ mg} \pm 2.09$ , posterior cortex left  $53.26 \text{ mg} \pm 1.83$ , anterior cortex right  $51.55 \text{ mg} \pm 1.95$ , posterior cortex

right 53.85 mg  $\pm$  2.03, medulla 50.48 mg  $\pm$  1.36, midbrain 81.75 mg  $\pm$  3.97, cerebellum 48.50 mg  $\pm$  1.32) displayed limited variability between animals.

## Cerebral blood flow

Since the cardiac index of mouse is  $\sim$  0.5 ml/g body wt/min (Janssen *et al*, 2002) and the mean weight of a 6 week old C57BL/6J mouse was 20 g, a perfusion flow rate of approximately 10 ml/min is required to adequately replace the animals own blood supply. Regional flow rates have been determined independently using autoradiography in the Sv129 and C57BL/6J mouse, and were shown to range between 1.12-1.8 ml/g/min (Maeda *et al*, 2000; Majid *et al*, 2000). After much optimisation, 10 ml/min was indeed determined to give a cerebral flow rate within these ranges. All of the selected brain regions appeared pale at the end of each perfusion, suggesting that all of the blood had been successfully washed out of the brain vasculature, thus leaving capillaries optimally exposure to the perfusate.

The radiolabelled tracer [ $^{14}$ C]-diazepam was used as a marker of cerebral blood flow, as demonstrated in previous studies using the *in situ* method (Takasato *et al*, 1984). The volume of distribution ( $V_d$ ) and unidirectional influx constant ( $K_{in}$ ) for this marker are displayed in Table 2 and Fig. 9. These values provide a linear relationship with time and a  $K_{in}$  of 1.37 ml/g/min which can be determined from the slope of the graph in Fig. 9.

	Time (min)	1	1.5	2
Mean $V_d$ (ml/g)		1.56	1.93	2.69
SEM		0.09	0.07	0.20

**Table 2.** Volume of distribution ( $V_d$ ) for [ $^{14}$ C]-diazepam in whole brain at perfusion times 1, 1.5 and 2 minutes.

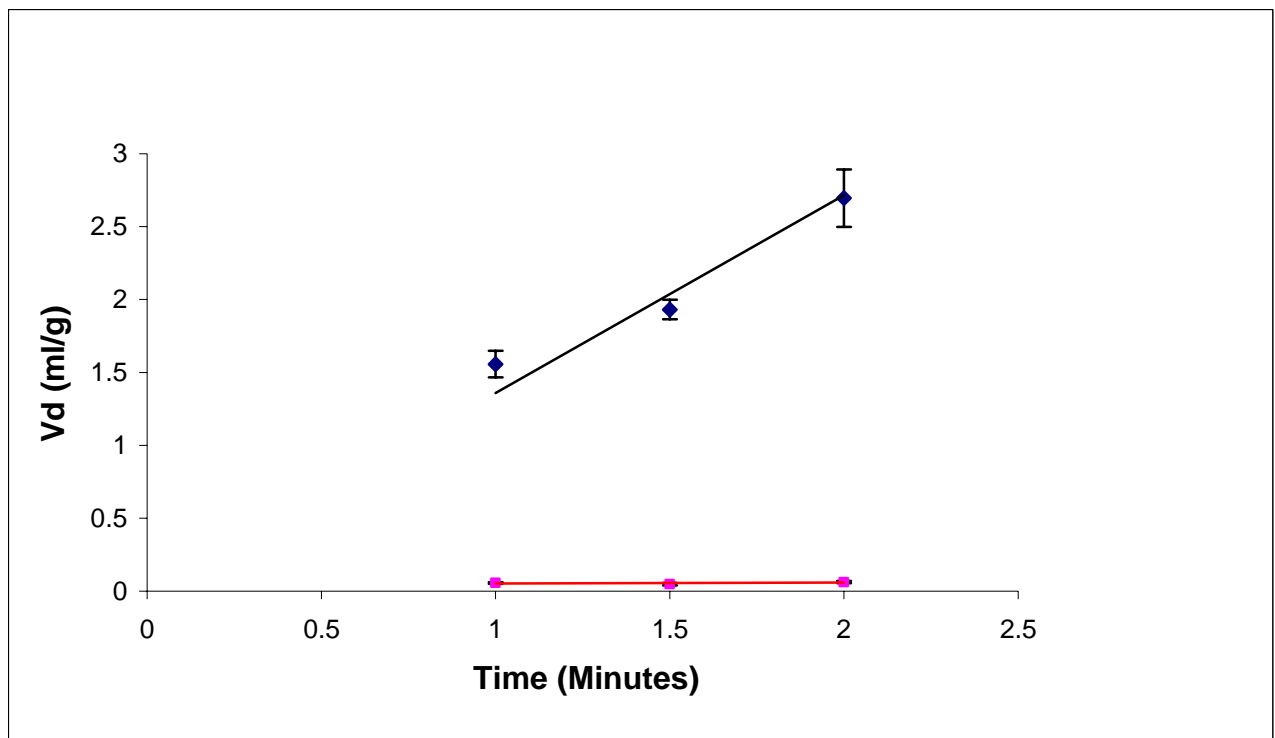


**FIG 9.** Graph of volume of distribution ( $V_d$ ) for diazepam (blue dots and black line) and sucrose (pink dots and red line) at perfusion times 1, 1.5 and 2 minutes. The unidirectional influx constant ( $K_{in}$ ) for diazepam can be determined from the slope of the graph.

$K_{in}$  was also subdivided into values for individual brain regions (Fig. 10). Regional differences were observed, with  $K_{in}$  greatest in OB (1.89 ml/g/min  $\pm$  0.3) and MED (2.29 ml/g/min  $\pm$  0.21), but lower in ACL (1.24 ml/g/min  $\pm$  0.11), PCL (0.91 ml/g/min  $\pm$  0.13), ACR (1.25 ml/g/min  $\pm$  0.16), PCR (0.95 ml/g/min  $\pm$  0.15), CER (1.25 ml/g/min  $\pm$  0.21) and MID (1.22 ml/g/min  $\pm$  0.14).  $K_{in}$  was largely comparable for different durations of perfusion.

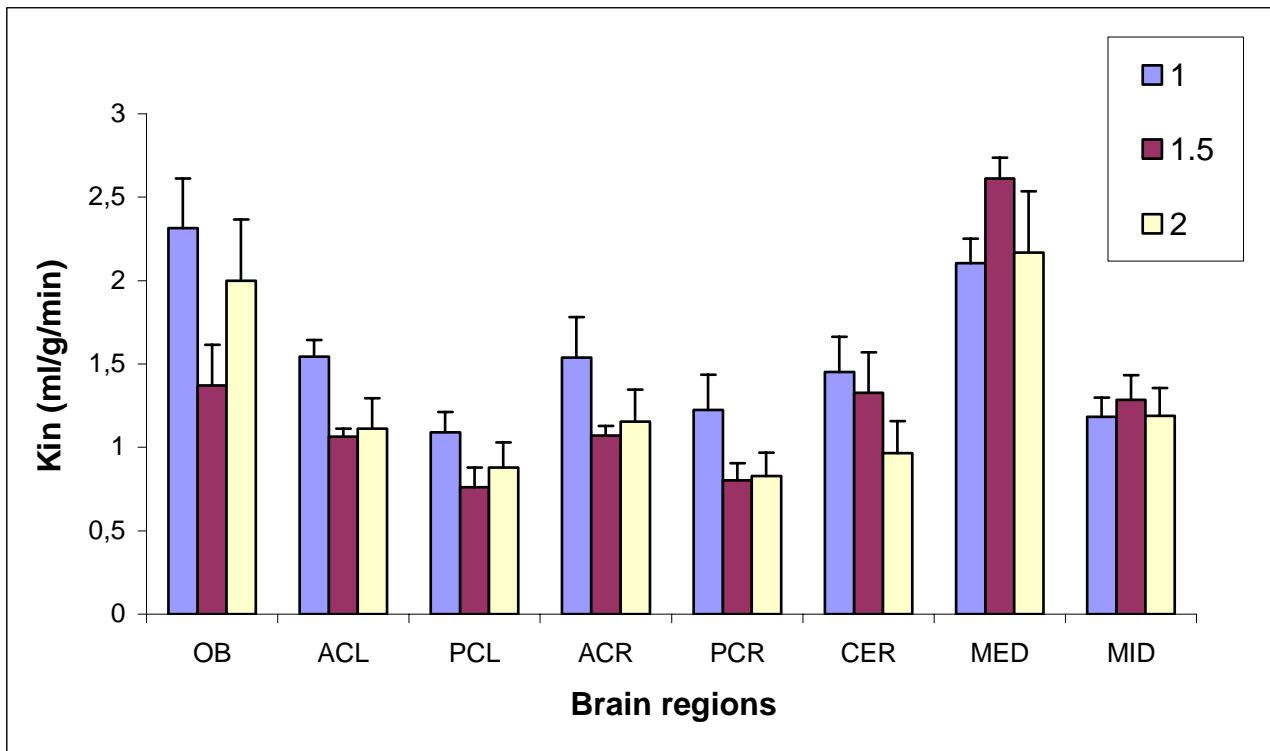


**FIG 10.** Unidirectional diazepam influx constant ( $K_{in}$ ) for individual brain regions at perfusion times 1, 1.5 and 2 minutes.

## Vascular space

$[^{14}\text{C}]$ -sucrose was used to assess vascular volume as it is a small radiolabelled tracer (189Da), but does not penetrate the BBB, unless it is defective (Drion *et al*, 1996; Dagenais *et al*, 2000).  $V_d$  was determined for this tracer at perfusion times 1, 1.5 and 2 minutes as displayed in Table 3 and Fig. 9.

	Time (min)	1	1,5	2
<b>Mean <math>V_d</math> (ml/g)</b>		0,057	0,048	0,062
<b>SEM</b>		0,005	0,009	0,008

**Table 3.** Volume of distribution ( $V_d$ ) for  $[^{14}\text{C}]$ -sucrose in whole brain at perfusion times 1, 1.5 and 2 minutes.

The graph is stationary for all durations of perfusion, and is in agreement with the rapidly equilibrating space filling within the first minute.  $V_d$  for  $[^{14}\text{C}]$ -sucrose was determined at

0.056ml/g  $\pm$  0.008, which was estimated from the y-intercept and therefore assumed to be the vascular volume in the 6 week old C57BL/6J mouse brain.

Capillary depletion data following a 2 minutes perfusion with [<sup>14</sup>C]-sucrose further confirmed that when brain capillaries and all major vessels were combined, the total volume is also ~5%.

## Excitatory amino acids

[<sup>3</sup>H]-glutamic acid and [<sup>3</sup>H]-glycine are carrier-mediated excitatory amino acids with low brain penetrance, so were used to investigate transporter function in the BBB. Figure 11 is a Michaelis-Menten plot representing BBB substrate kinetics for [<sup>3</sup>H]-glutamic acid in whole brain. There is a linear increase in substrate velocity with increasing concentration of unlabelled glutamic acid up until 225  $\mu$ mol/L where the transport system begins to saturate.  $K_m$  and  $V_{max}$  were estimated at 229.3  $\mu$ mol/L and 8.041 nmoles/min respectively.

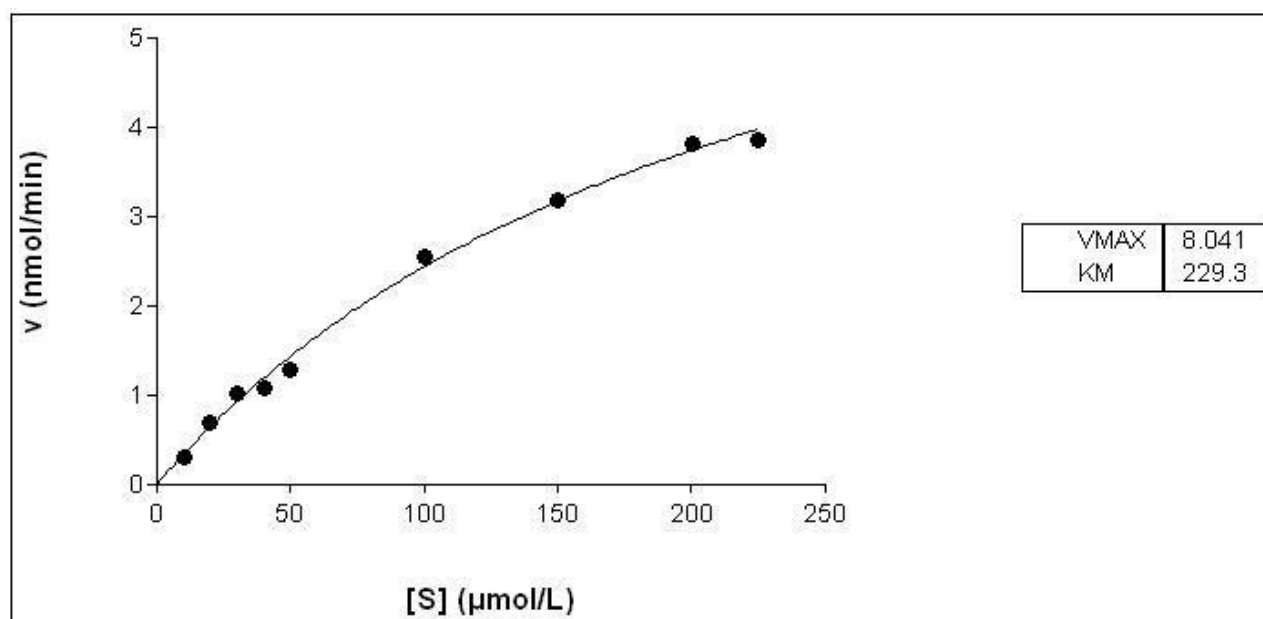


**FIG 11.** Michaelis-Menten plot representing BBB substrate kinetics for [<sup>3</sup>H]-glutamic acid in whole brain.

Substrate kinetics for selected brain regions (OB, CTX, CB, MED, MID) are presented in table 4.

		OB	CTX	CB	MED	MID
$V_{max}$ (nmoles/min)		10.75	8.354	12.66	10.39	7.306
$K_m$ ( $\mu\text{mol/L}$ )		281.1	372.9	365.1	191.6	182.1

**TABLE 4.** Substrate kinetics for [ $^3\text{H}$ ]-glutamic acid in selected brain regions.

A Michaelis-Menten plot has also been generated for [ $^3\text{H}$ ]-glycine in whole brain (Fig. 12). [ $^3\text{H}$ ]-glycine has a far greater brain penetrance than [ $^3\text{H}$ ]-glutamic acid, with a linear component exceeding 19.7 nmoles/min at 1500  $\mu\text{mol/L}$ .  $K_m$  was estimated at 1462  $\mu\text{mol/L}$  and  $V_{max}$  at 40.31 nmoles/min.

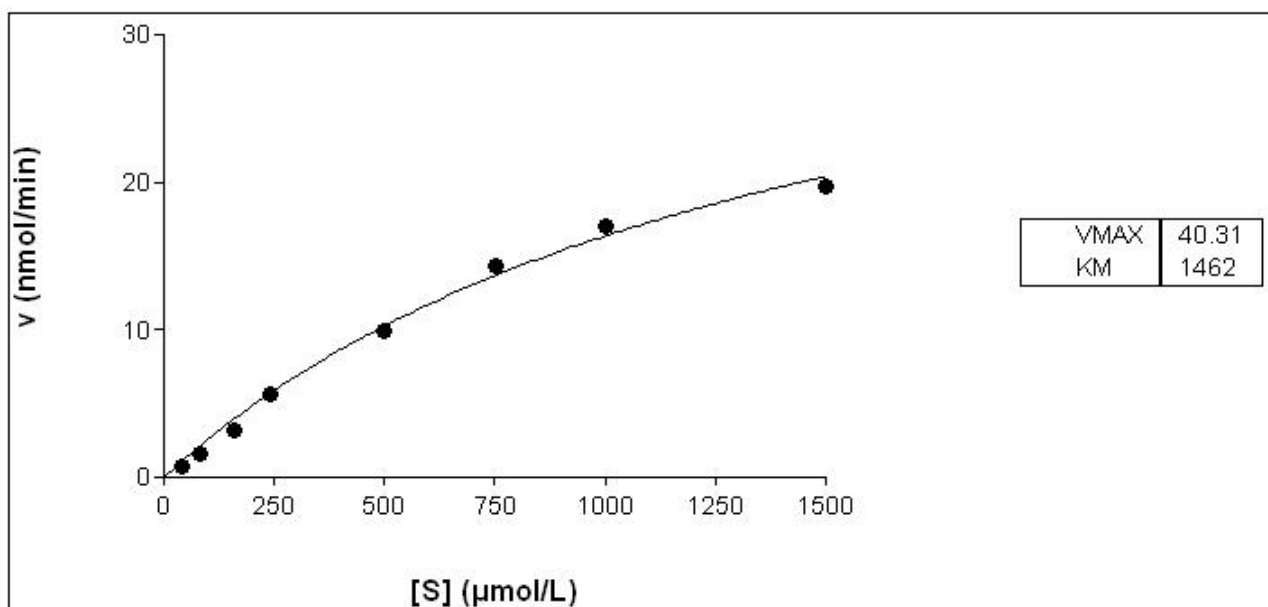


**FIG 12.** Michaelis-Menten plot representing BBB substrate kinetics for [ $^3\text{H}$ ]-glycine in whole brain.

Values for individual brain regions are summarized in table 5.

		OB	CTX	CB	MED	MID
$V_{max}$ (nmoles/min)		38.21	25.23	59.54	57.79	33.70
$K_m$ ( $\mu\text{mol/L}$ )		808.8	1004	1872	1293	1039

**TABLE 5.** Substrate kinetics for [ $^3\text{H}$ ]-glycine in selected brain regions.

## Electron microscopical analyses

For ultrastructural assessment of blood vessel permeability, the *in situ* brain perfusion technique was also employed to fix mice brain with lanthanum nitrate in the fixative solution, and then the tight junctions were examined more closely using electron microscopy. Lanthanum nitrate is readily detectable as a black precipitate, which enabled us to discriminate between tracer in the endothelial lumen, interendothelial cleft and that which has passed through the endothelial cells into the parenchyma. From preliminary results in the brain of wild type C57BL/6 mice we demonstrated

that the vessels remain tight, even to a well accepted electron microscopical tracer during the course of the perfusion (Fig. 13).

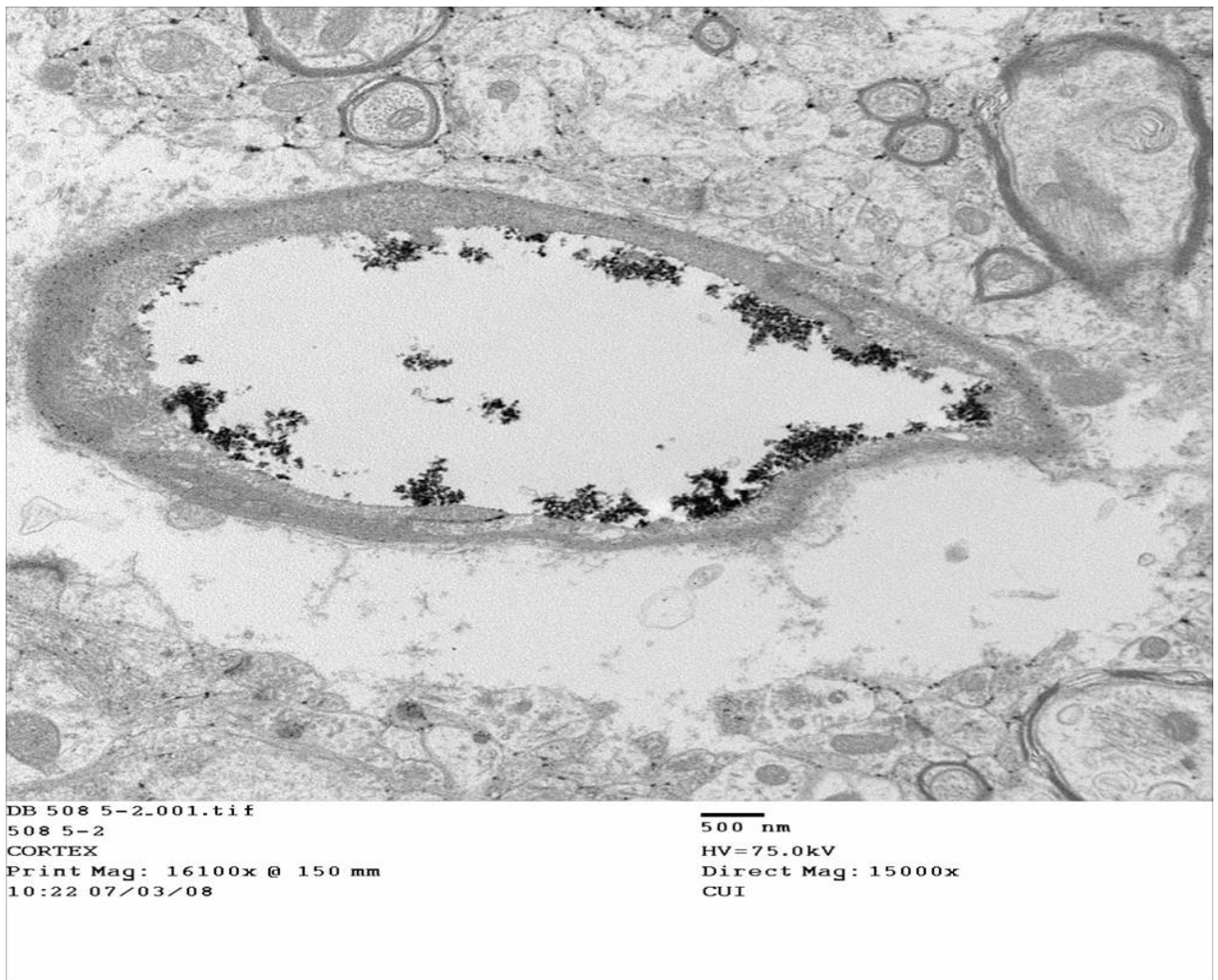


**FIG 13.** Electron microscopical image of a section of a wild type C57BL/6 cortex. The black precipitate represents the lanthanum nitrate which is readily detectable just in the endothelial lumen.

## Sanfilippo type IIIA mice

The *in situ* brain perfusion technique was widely employed for looking into the BBB in MPS IIIA mice and their respective control strains of mouse, at 4-6 and 8-10 months of age.

At 4-6 months of age, [<sup>14</sup>C]-sucrose revealed a significant reduction in vascular volume of Sanfilippo mice (Fig. 14).

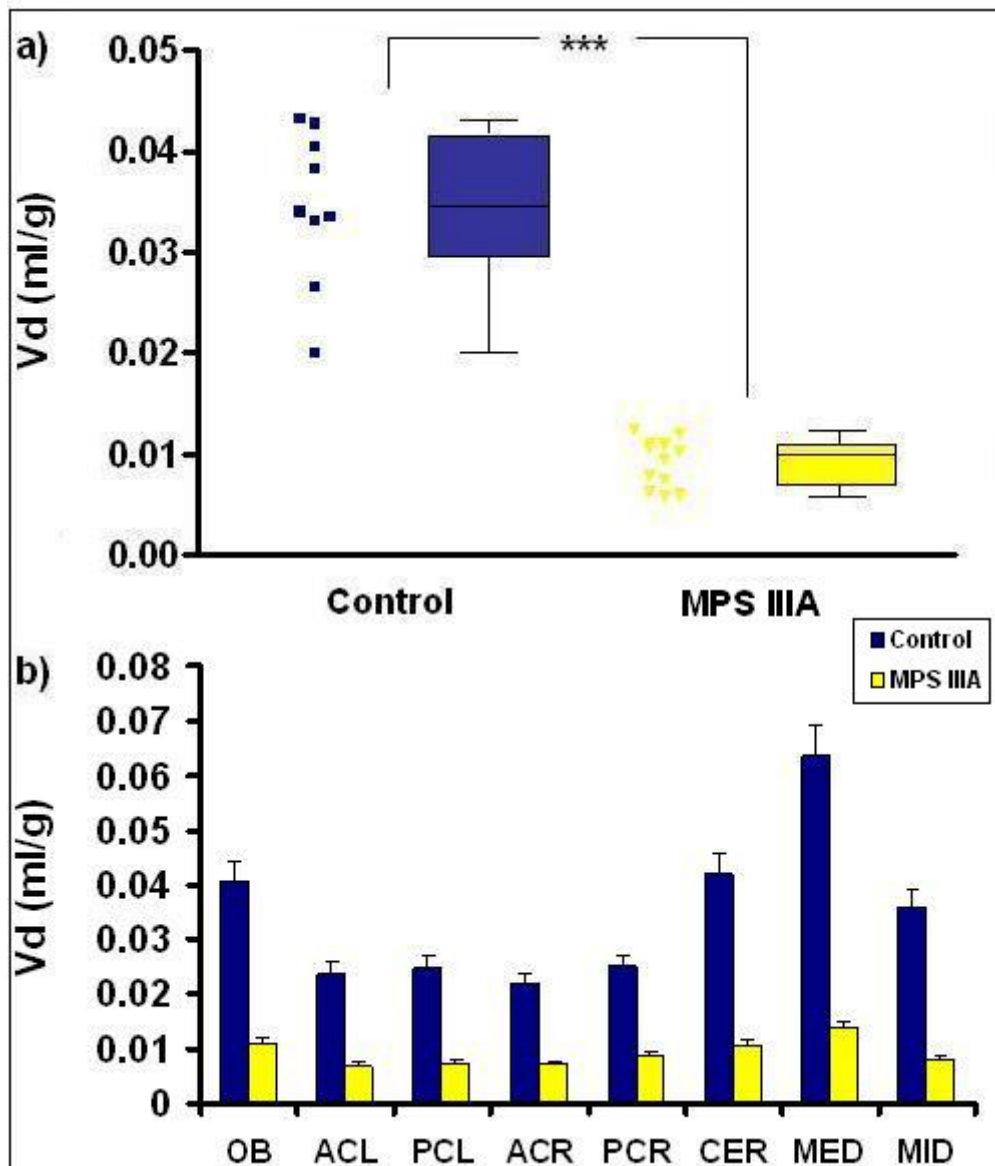


**FIG 14.** Volume of distribution ( $V_d$ ) in whole brain (a) and regions (b), measured with [<sup>14</sup>C]-sucrose as a vascular marker in MPS IIIA and control mice at 4-6 months of age.

The perfusate flow, as assessed from the  $K_{in}$  for [ $^{14}$ C]-diazepam, was increased in mutant mice compared to control mice (Fig. 15).

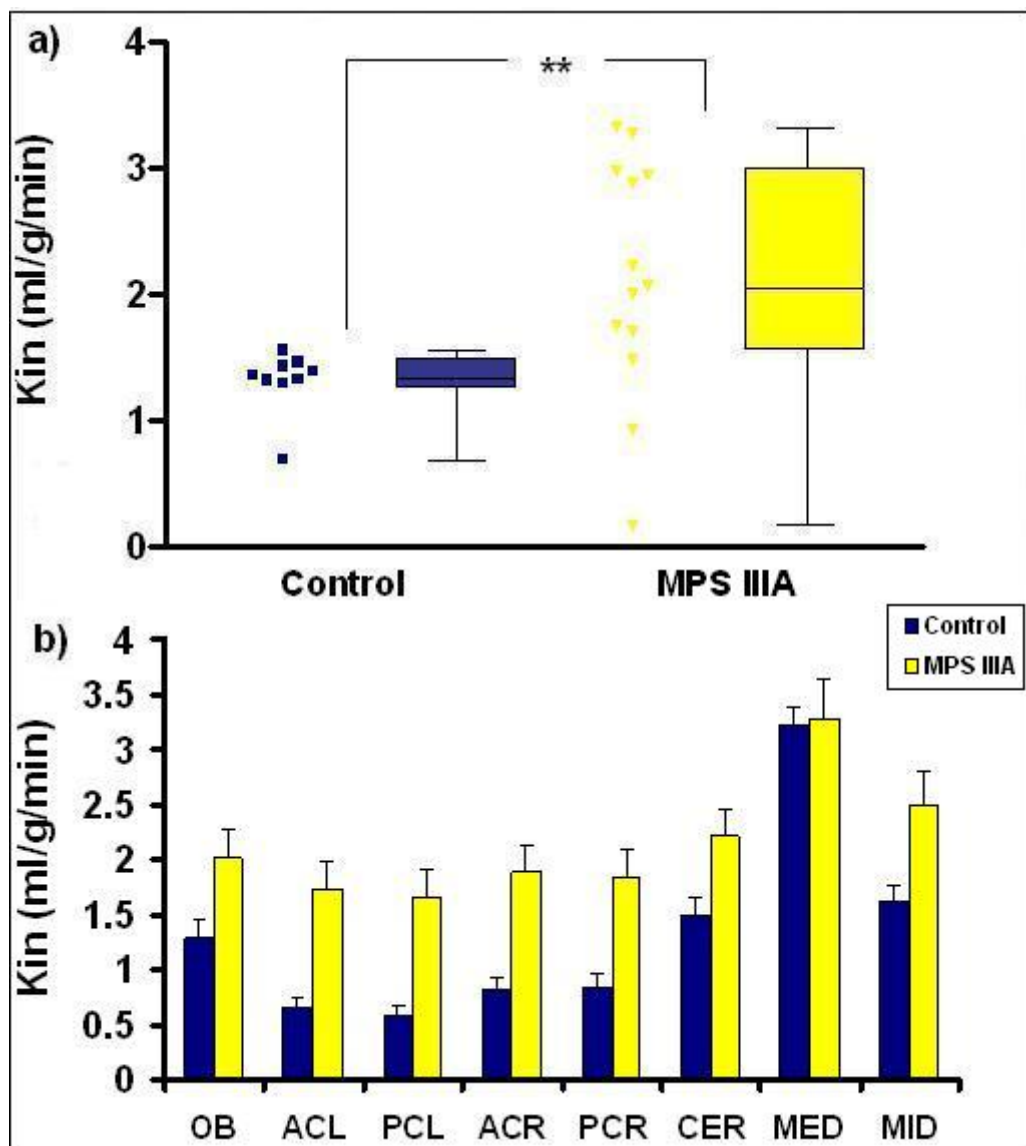


**FIG 15.** Unidirectional influx constant ( $K_{in}$ ) for whole brain (a) and regions (b), measured with [ $^{14}$ C]-diazepam as a marker of perfusate flow in MPS IIIA and control mice at 4-6 months of age.

The carrier-mediated substances with low brain penetrance revealed different trends, with  $K_{in}$  for [ $^3$ H]-glycine significantly increased in MPS mice (Fig. 16) while the  $K_{in}$  for [ $^3$ H]-glutamic acid and [ $^3$ H]-tyrosine remained unchanged between phenotypes (Fig. 17).

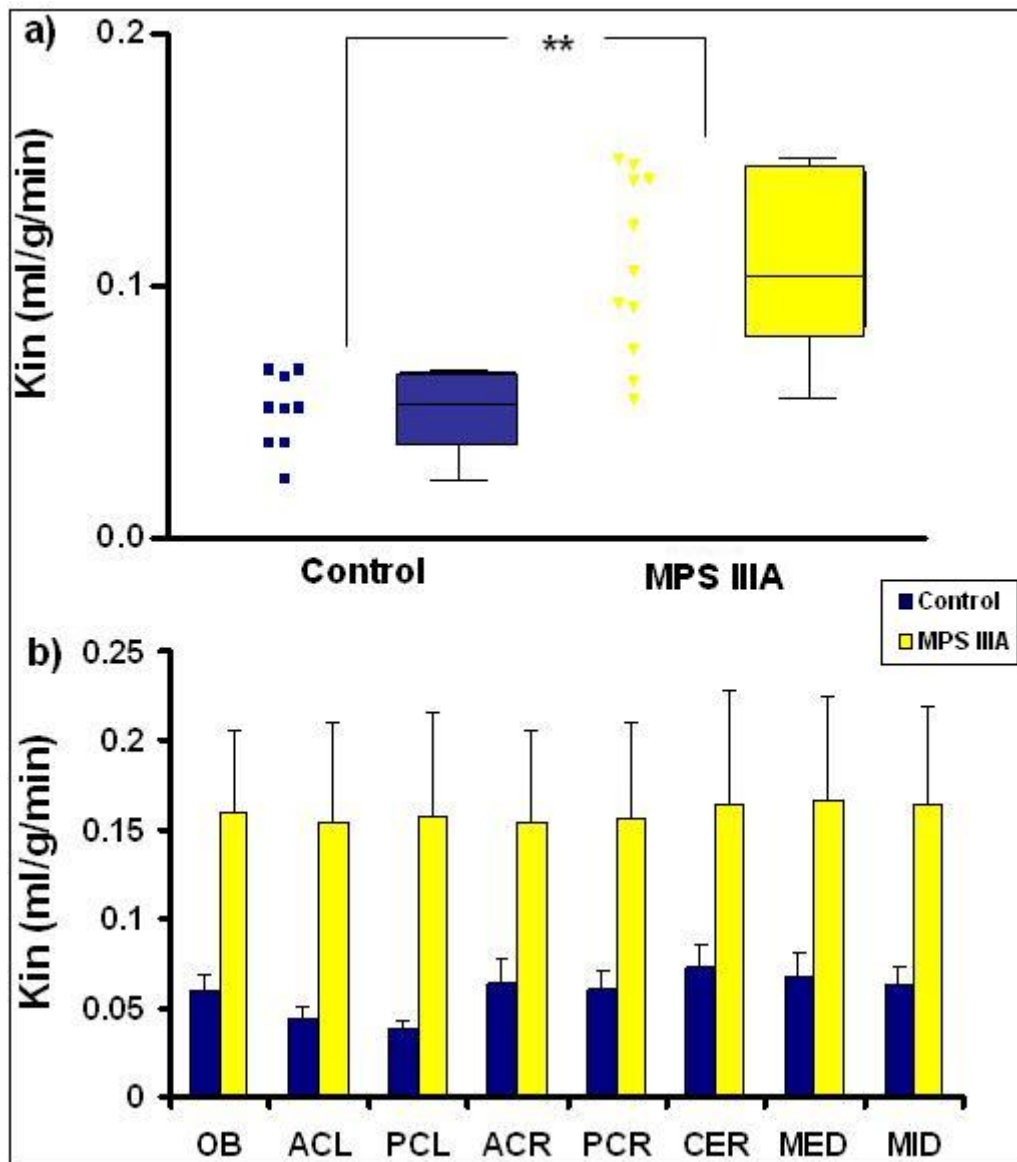


**FIG 16.** Unidirectional influx constant ( $K_{in}$ ) for whole brain (a) and regions (b), measured with [ $^3$ H]-glycine as a carrier-mediated substrate in MPS IIIA and control mice at 4-6 months of age.

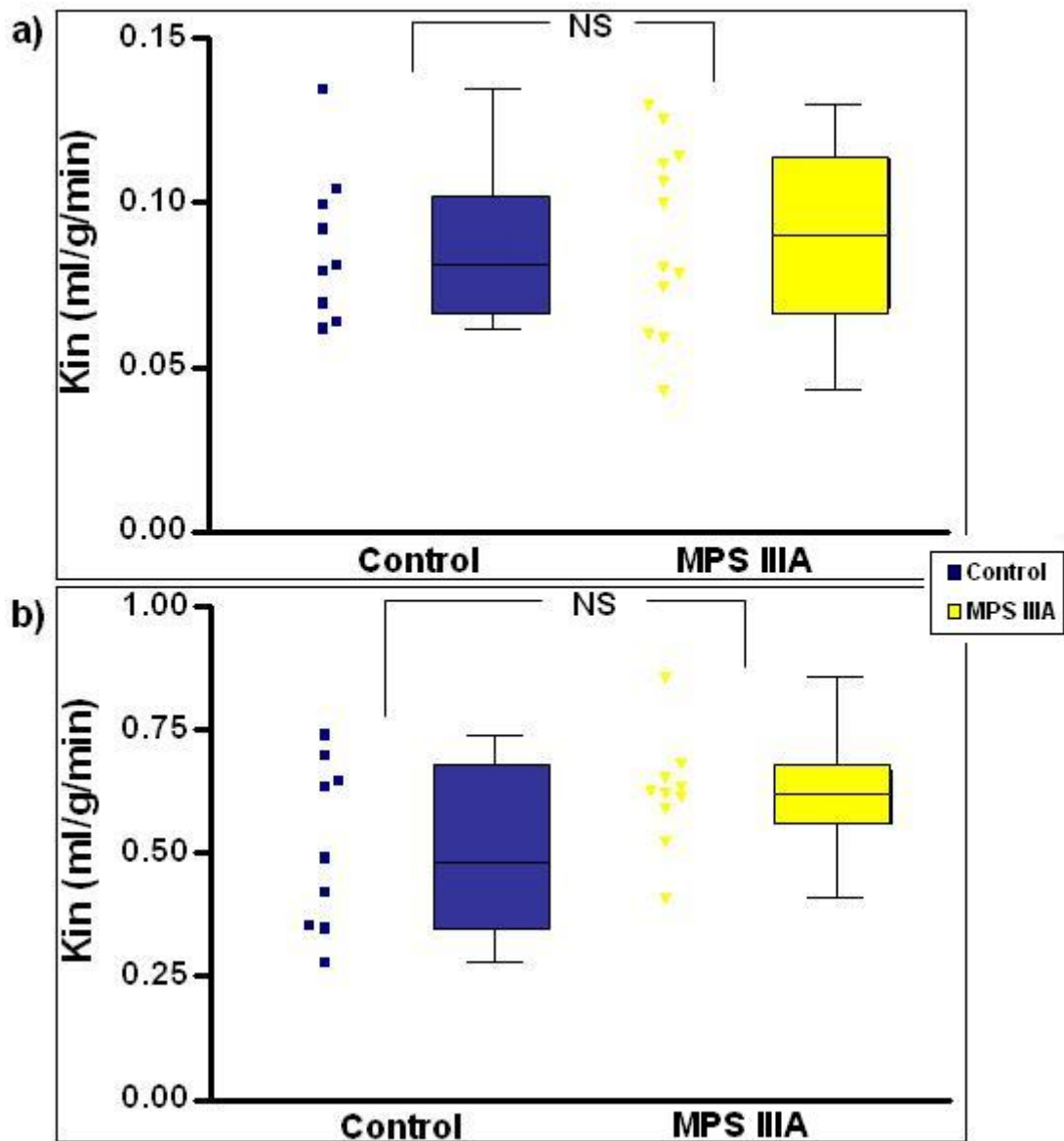


**FIG 17.** Unidirectional influx constant ( $K_{in}$ ) for whole brain, measured with [ $^3\text{H}$ ]-glutamic acid (a) and [ $^3\text{H}$ ]-tyrosine (b) as carrier-mediated substrates in MPS IIIA and control mice at 4-6 months of age.

At 8-10 months of age, the difference between volume of distribution for [ $^{14}\text{C}$ ]-sucrose in Sanfilippo mice and their controls became not significant (Fig. 18) while the  $V_d$  assessed from [ $^3\text{H}$ ]-inulin, another marker of vascular volume (Takasato *et al*, 1984; Dagenais *et al*, 2000), revealed a significant reduction in mutants (Fig. 19).

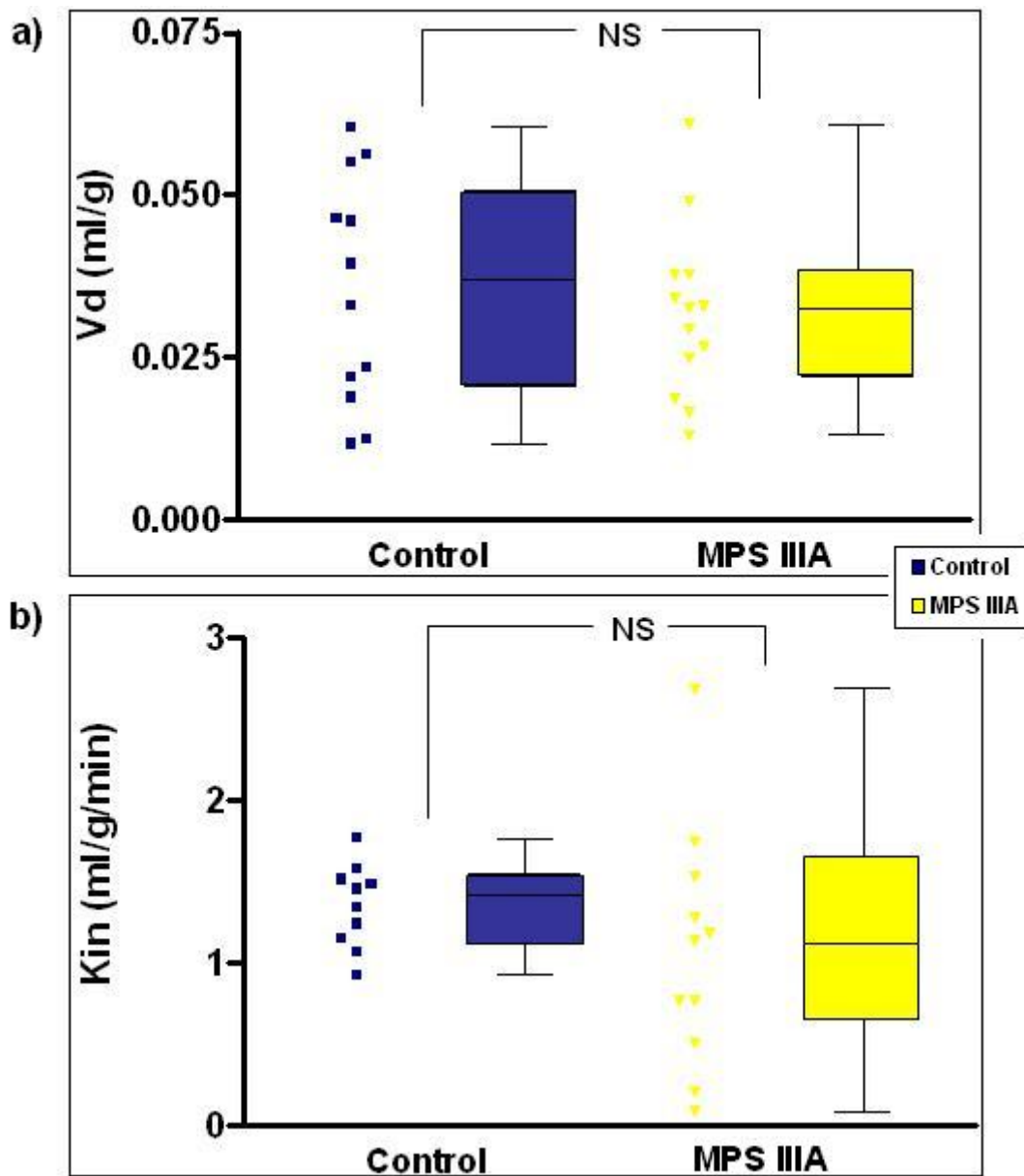


**FIG 18.** Volume of distribution ( $V_d$ ) measured with [ $^{14}$ C]-sucrose as a vascular marker (a) and unidirectional influx constant ( $K_{in}$ ) measured with [ $^{14}$ C]-diazepam as a marker of perfusate flow (b), for whole brain in MPS IIIA and control mice at 8-10 months of age.

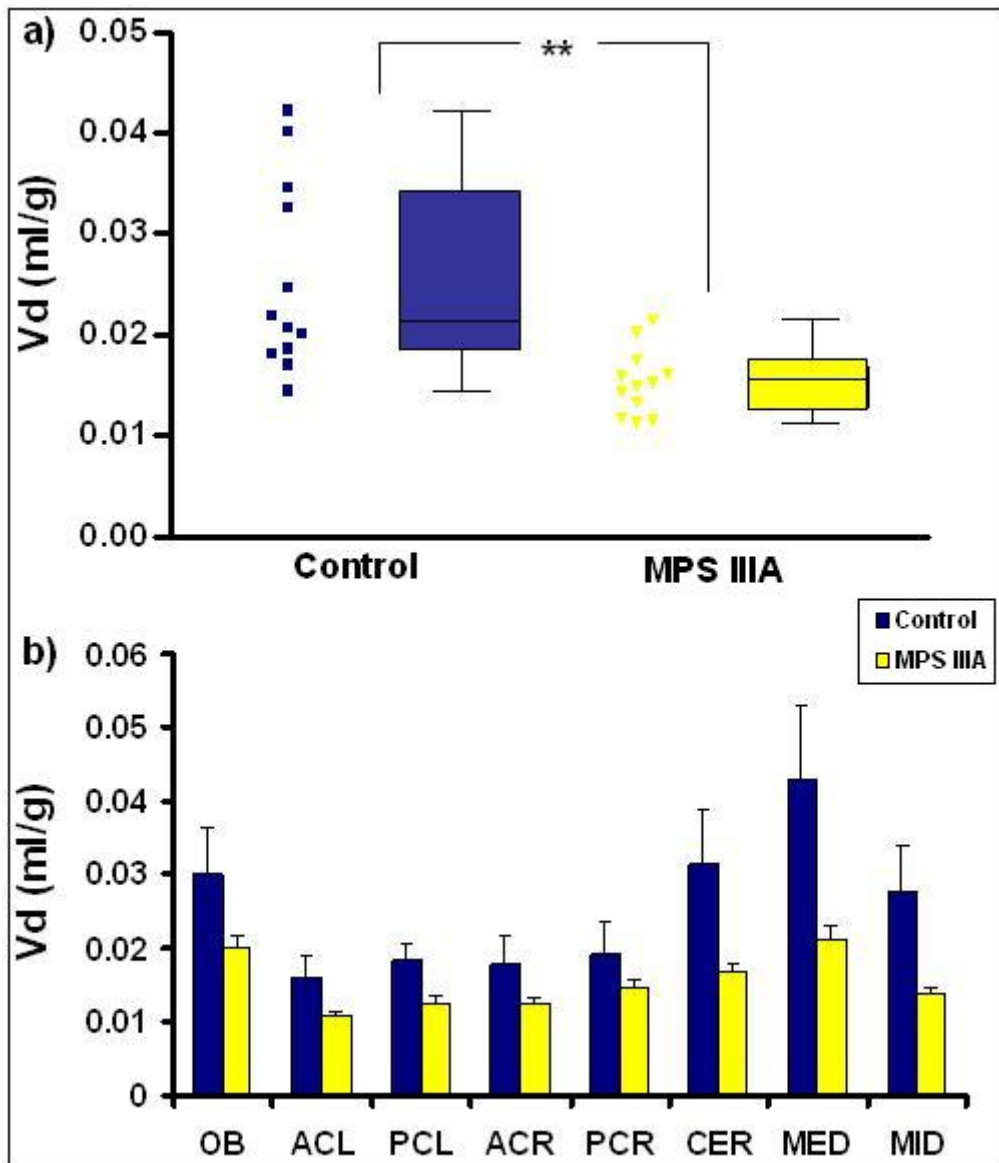


**FIG 19.** Volume of distribution ( $V_d$ ) in whole brain (a) and regions (b), measured with [ $^3\text{H}$ ]-inulin as a vascular marker in MPS IIIA and control mice at 8-10 months of age.

Also the difference between  $K_{in}$  for [ $^{14}\text{C}$ ]-diazepam in MPS mice and their controls became not significant (Fig. 18).

$K_{in}$  for [ $^3\text{H}$ ]-glycine remained significantly increased in mutants at this age (Fig. 20) and  $K_{in}$  for [ $^3\text{H}$ ]-glutamic acid and [ $^3\text{H}$ ]-tyrosine still unchanged between phenotypes.

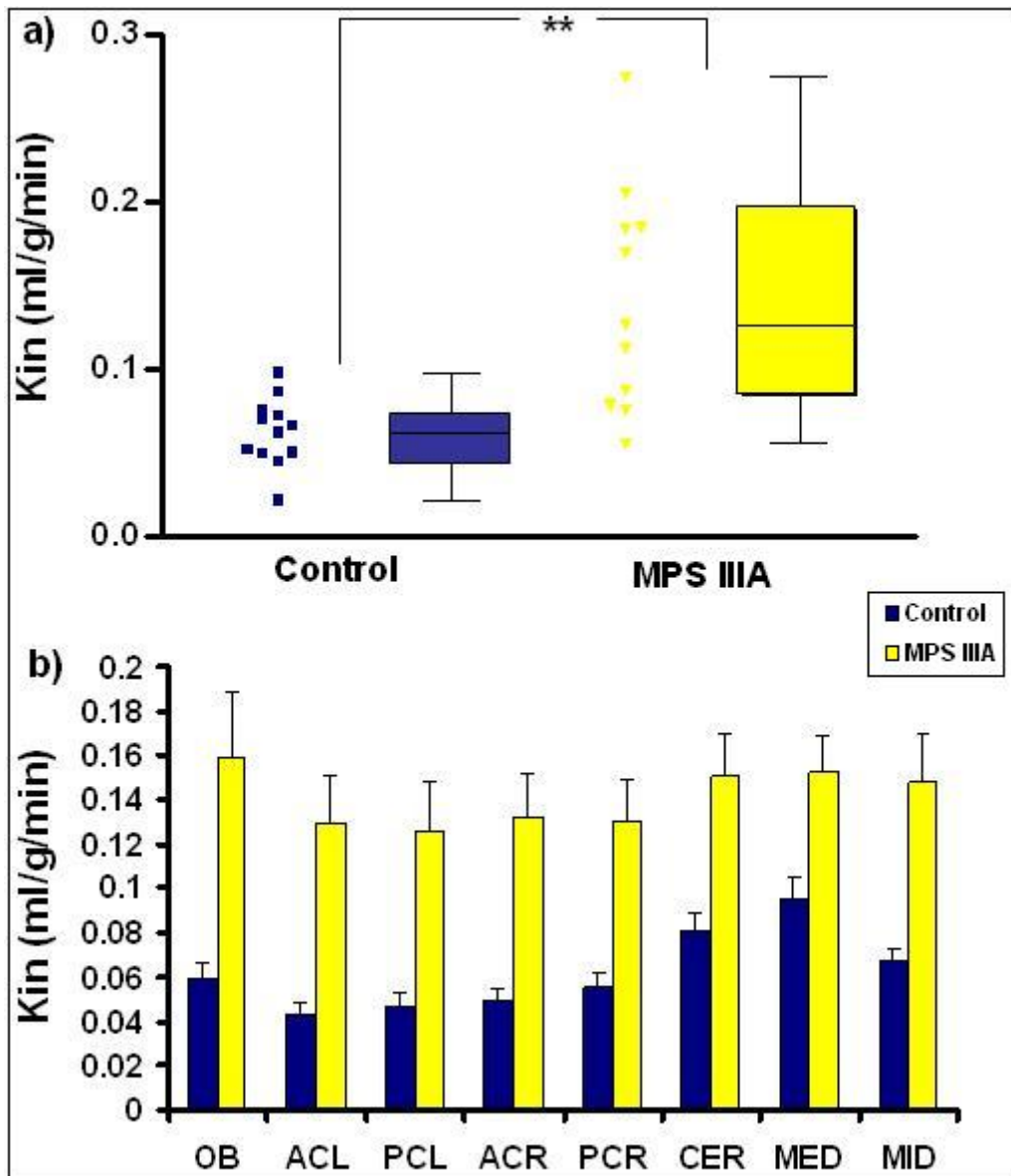


**FIG 20.** Unidirectional influx constant ( $K_{in}$ ) for whole brain (a) and regions (b), measured with [ $^3\text{H}$ ]-glycine as a carrier-mediated substrate in MPS IIIA and control mice at 8-10 months of age.

### Sanfilippo type IIIB mice

Initial findings from perfusions were obtained for MPS IIIB mice and their respective control strains of mouse, at 4-6 and 8-10 months of age.

[ $^{14}\text{C}$ ]-sucrose revealed a similar trend to that in Sanfilippo A mice with a volume of distribution significantly reduced at 4-6 months of age in Sanfilippo B mice (Fig. 21) and not significant difference between phenotypes at 8-10 months of age (Fig. 22).

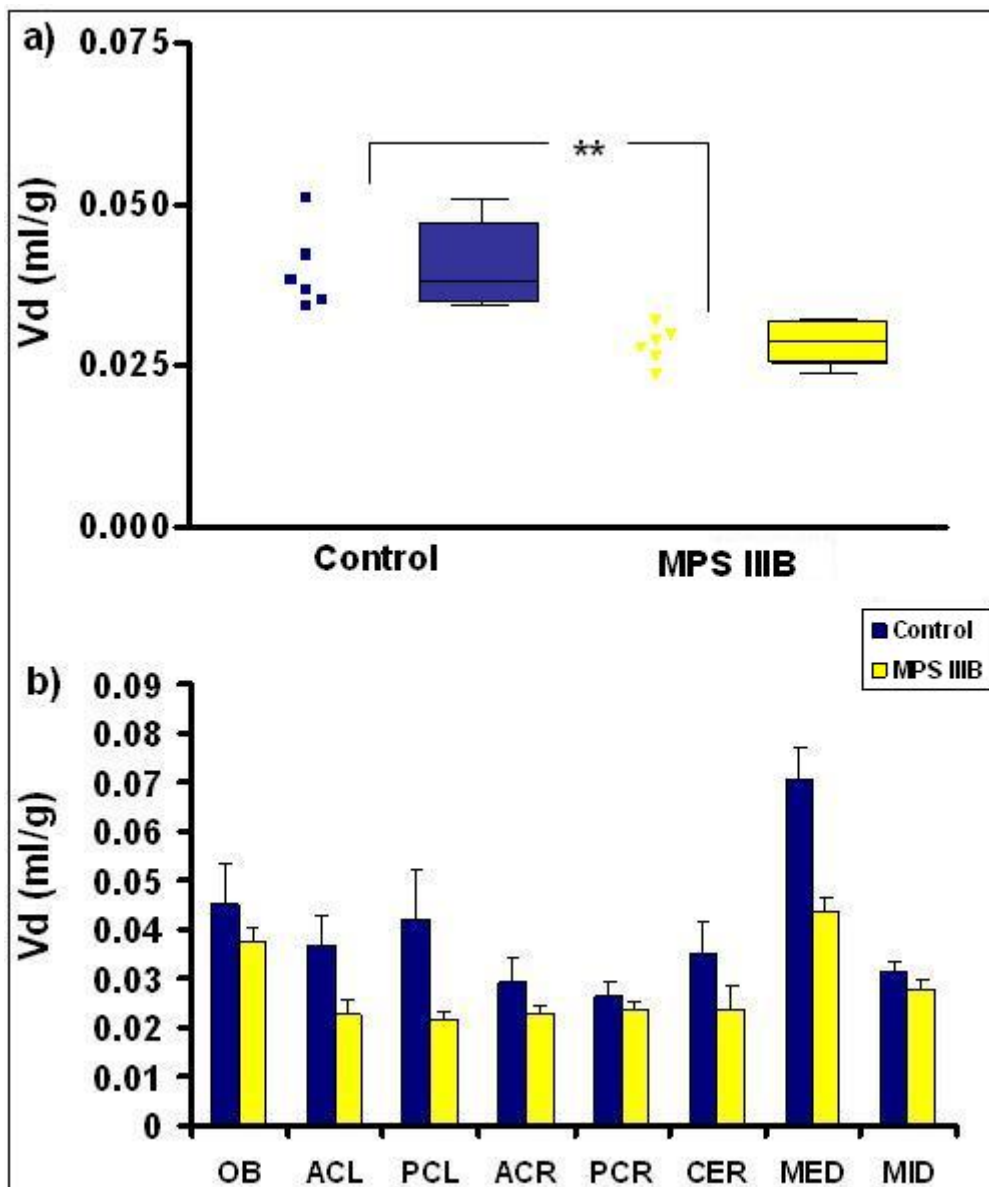


**FIG 21.** Volume of distribution ( $V_d$ ) in whole brain (a) and regions (b), measured with [ $^{14}\text{C}$ ]-sucrose as a vascular marker in MPS III B and control mice at 4-6 months of age.

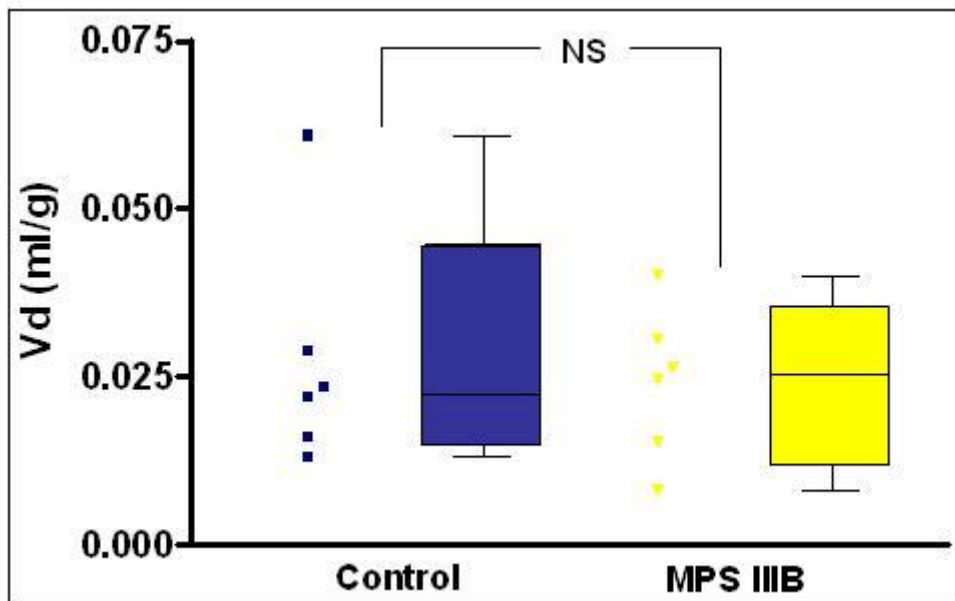


**FIG 22.** Volume of distribution ( $V_d$ ) in whole brain measured with [ $^{14}\text{C}$ ]-sucrose as a vascular marker in MPS III B and control mice at 8-10 months of age.

Preliminary data for [ $^{14}\text{C}$ ]-diazepam showed not significant difference between mutants and controls at both the ages.

Also  $K_{in}$  for [ $^3\text{H}$ ]-glycine and [ $^3\text{H}$ ]-glutamic acid didn't revealed a significant difference between phenotypes at 8-10 months of age (Fig. 23).

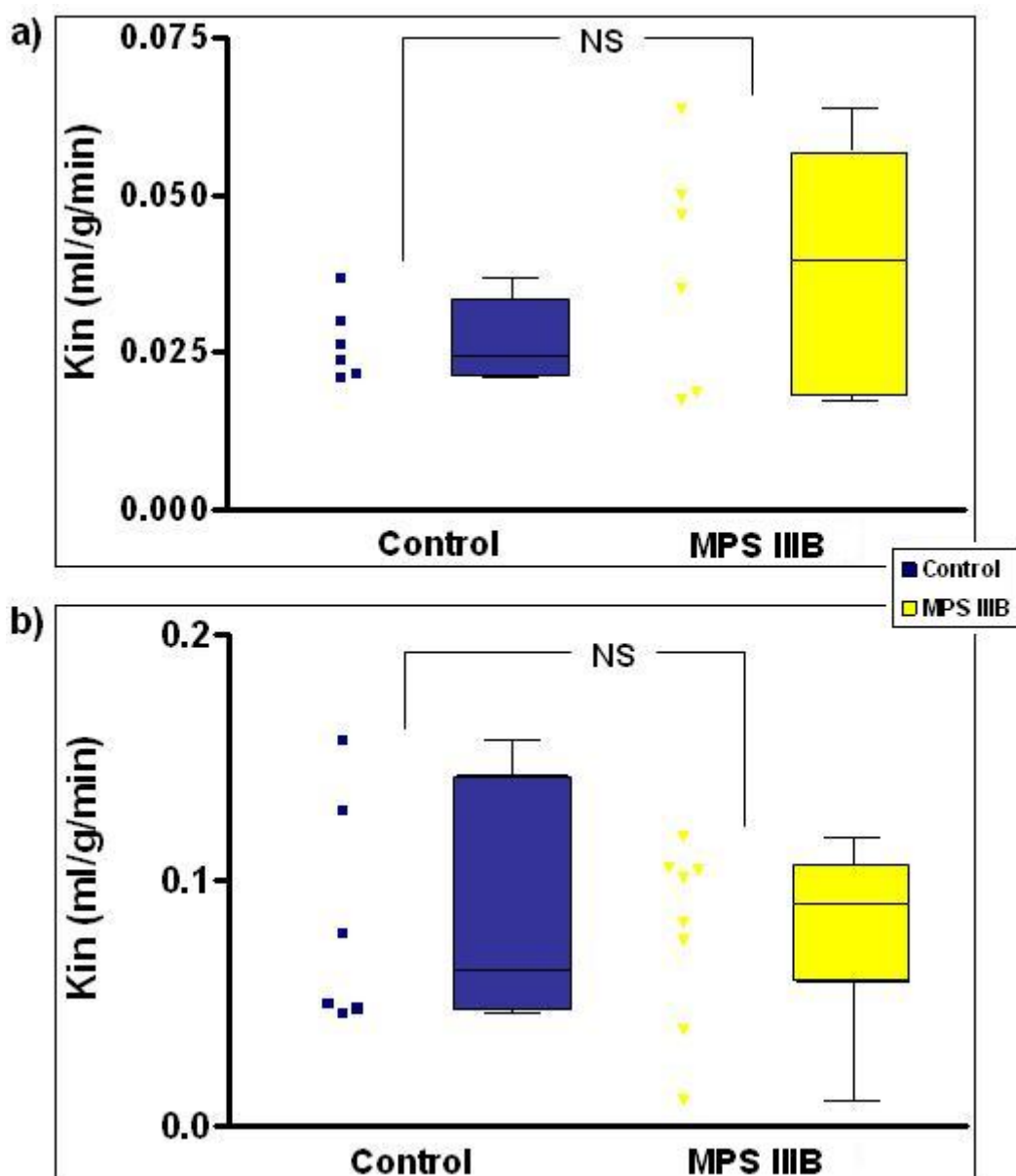


**FIG 23.** Unidirectional influx constant ( $K_{in}$ ) for whole brain, measured with [<sup>3</sup>H]-glycine (a) and [<sup>3</sup>H]-glutamic acid (b) as carrier-mediated substrates in MPS III B and control mice at 8-10 months of age.

### Intraperitoneal injections

Perfusion times 1, 2 and 3 minutes were found to be not long enough to assess brain uptake of [<sup>3</sup>H]- NB-DNJ, so this compound was employed for intraperitoneal injections in mice and evaluated for times up to 60 minutes. In this case, where there may be some variation in the  $C_{pl}$  during the experiment, the area under plasma concentration time curve (Fig. 24) was considered to calculate  $K_{in}$ .

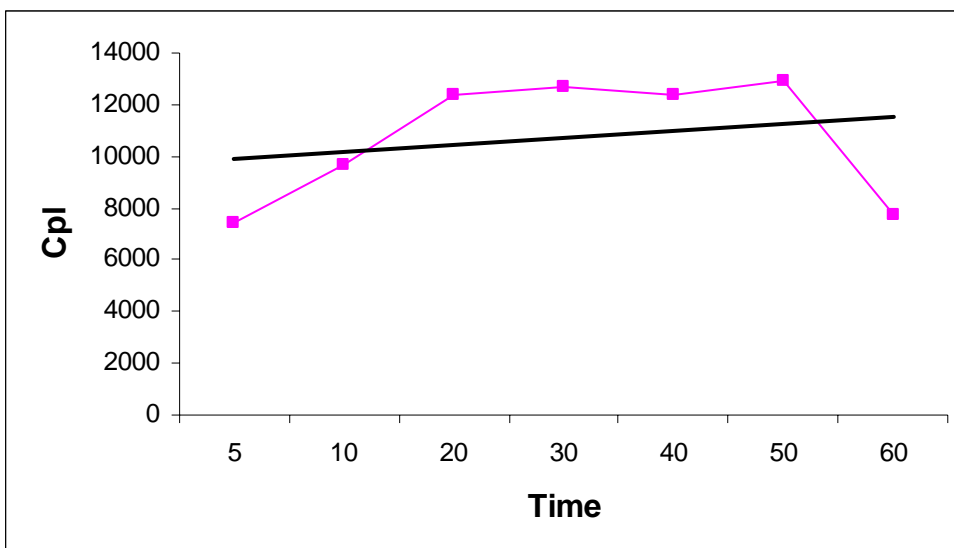


**FIG 24.** Variation in the  $C_{pi}$  at different times (in minutes in the figure). Area under plasma concentration time curve was considered to calculate  $K_{in}$ .

The unidirectional transfer constant  $K_{in}$  demonstrated that Zavesca® crossed the BBB, very slowly but progressively (Fig. 25).

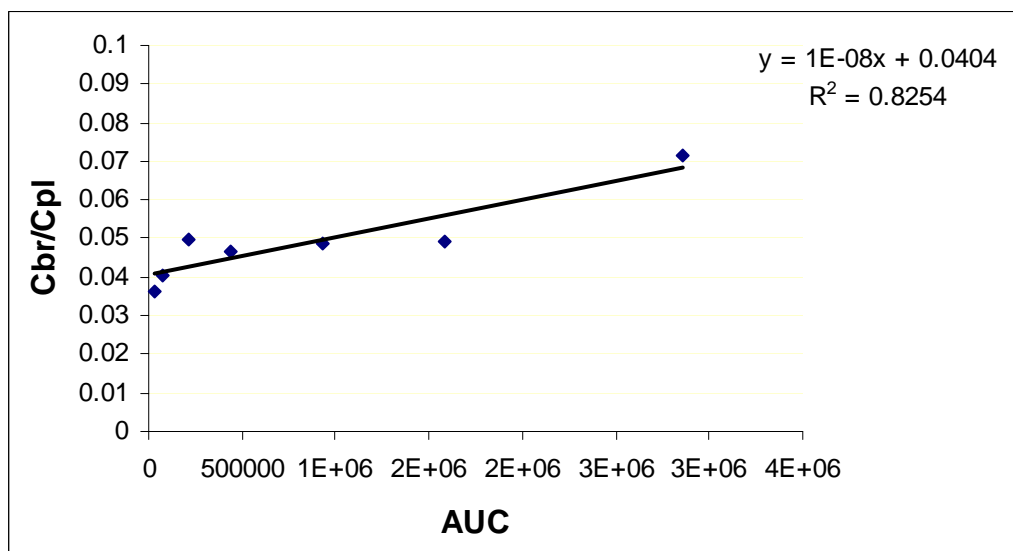


**FIG 25.** Unidirectional influx constant ( $K_{in}$ ) for whole brain measured with [<sup>3</sup>H]- NB-DNJ in 6 weeks wild type C57BL/6 mice.

## DISCUSSION

Sanfilippo syndrome is the most common form of MPS, a group of rare genetic diseases, and is caused by deficiency in enzymes that degrade the glycosaminoglycan heparan sulphate, with consequent harmful and progressive accumulation in lysosomes of this big molecule and additional molecules, as GM2/GM3 gangliosides, whose degradation could be reduced or inhibited by the main storage. Patients with MPS III have marked central nervous system involvement, as do up to 70% of other lysosomal storage diseases.

Despite important therapies available for LSD, like ERT, pathologies with CNS degeneration are not feasibly treated because of the blood-brain barrier. A few options, not disrupting the BBB, seem to be represented by small molecules therapies, believed to cross the BBB, useful just in diseases caused by mutant but yet catalytically active enzymes; or transplantation, like BMT, successful at reversing neuropathology in some LSDs and not in others, as in MPS III.

Furthermore there is evidence that in some of the lysosomal storage disorders the function of the blood-brain barrier itself is compromised perhaps leading directly to further cascade processes resulting in neuropathology. The specific impact of this secondary event on the initiation and the progression of the neurodegenerative process is currently poorly understood.

Thus the aim of the present PhD project was a better understanding of the BBB functions under physiological conditions as well as during a diseased state by setting up a system to study the barrier and determining whether changes to the BBB occur in Sanfilippo Syndrome, in order to finally develop successful new and improved drugs that may repair and cross the BBB to treat the CNS.

This project was conducted at King's College London where the *in situ* brain perfusion technique was well-known and therefore refined to achieve the purpose.

Several alternative methods exist, but the *in situ* brain perfusion technique offers superior sensitivity over other tracer based methods and can be used to precisely quantify the transport of solutes across the BBB (Takasato *et al*, 1984 and Begley 1999).

This technique has been readily used to investigate the BBB in the Guinea pig (Zlokovic *et al*, 1986), rat (Takasato *et al*, 1984) and more recently in the mouse (Drion *et al*, 1996; Dagenais *et al*, 2000; Murakami *et al*, 2000; Urayama *et al*, 2004 and LaRue *et al*, 2004); and it was decided to refine this well-established method in the mouse as evidence suggests that mouse strains have variation between individuals in the completeness of the vascular circle of Willis supplying the

brain (Ward *et al*, 1990), thus this would imply that a standard intra-carotid perfusion would not be sufficient to adequately supply all regions of the rodent brain.

The initial challenge was to modify the method sufficiently to allow an adequate flow to all parts of the brain, whilst being careful not to compromise the integrity of the BBB. With this in place the modified *in situ* brain perfusion technique would provide a more accurate platform to assess transport of solutes across the BBB. A transcardiac approach was therefore adopted, with the descending aorta tied off so that only the upper half of the body would be perfused by directly entering the base of the heart via the left ventricle, thus the carotid artery would be supplied before it bifurcates (Fig. 26).

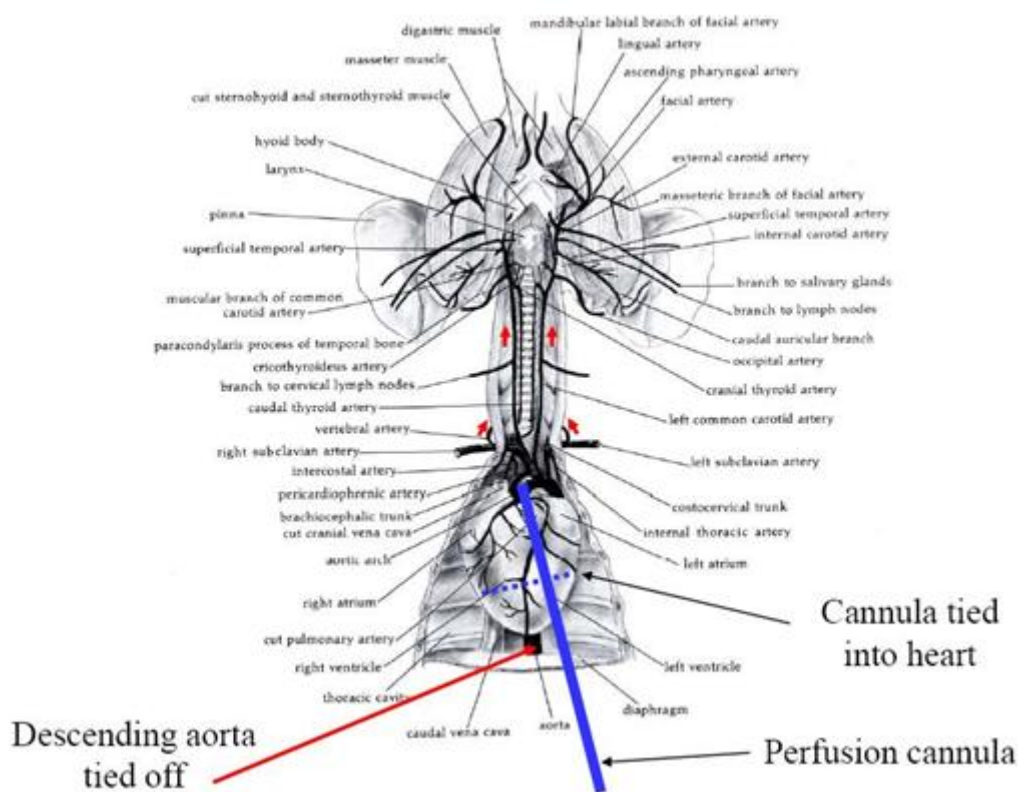


**FIG 26.** Modified cannula placement which allows the entire brain to be perfused.

It became then apparent that the flow rate of 2 ml/min used by Urayama *et al*. (2004) was a gross underestimation of physiological flow in the mouse. Indeed, as the cardiac index of the mouse is ~ 0.5 ml/g body wt/min (Janssen *et al*, 2002), this suggests that the flow rate would have to be increased by ~ 5 fold in order to supply an adequate rate of perfusate flow to brain tissue as the mean weight of a 6 week old C57BL/6J mouse was 20 g. The delivery of perfusate was achieved after much experimentation and a perfusion flow rate of 10 ml/min was consistent with blood flow measured in the intact animal by alternative methods (Maeda *et al*, 2000 and Majid *et al*,

2000). In these studies [<sup>14</sup>C]-iodoantipyrine was administered intraperitoneally (Maeda *et al*, 2000), or via the right femoral artery (Majid *et al*, 2000) and tissue radioactivity was assayed by quantitative autoradiography. In contrast, our study measured [<sup>14</sup>C]-diazepam uptake, another flow limited substrate which can be used to estimate cerebral perfusion rate (Takasato *et al*, 1984).

In addition to the careful adjustment of flow and positioning of the cannula for perfusion, the sufficient duration that the perfusion would run for needed to be found. Mice were initially perfused for 1, 1.5 and 2 minutes before the brain was removed, sectioned and assessed for penetrance of solutes. The typical system pressure obtained from the pressure transducer had an initial peak followed by a decline after ~ 20 seconds. This is likely to represent viscous blood being washed out of the system followed by a plateau whilst perfusate is circulating. For this reason perfusions were not conducted for less than 1 min as it makes extrapolation of data during this period unreliable and inaccurate. Indeed, the majority of perfusions were conducted for 2 minutes, which provided more than adequate time to allow blood to run clear from circulation and for the solute to be distributed. The brain is left pale if all the blood is washed out during the perfusion. The mouse brains were always found to be totally pale after each perfusion which suggested that the flow rate, positioning of cannula, and duration of perfusion were sufficient to supply all regions of the brain.

Several parameters were then investigated to determine whether the *in situ* brain perfusion method may be applied to the mouse without disturbance to the physical or functional integrity of the BBB. These parameters included the measurement of cerebral perfusion flow, brain vascular volume, and carrier-mediated transport of excitatory amino acids glutamic acid and glycine. Electron microscopy studies with lanthanum nitrate were also performed to assess whether the tight junctions became leaky during the course of perfusion.

A systolic pressure in excess of 126 mmHg is required to induce leakiness of the BBB (Rapoport 1976 and Hardebo *et al*, 1981). The pressure traces registered during perfusion remained between 40-80 mmHg, thus the flow rate was unlikely to cause damage to the BBB.

Brain vascular volume was assessed with [<sup>14</sup>C]-sucrose and perfusions were performed over a range of times, which allowed to determine whether this compound had a  $K_{in}$  and thus movement into the brain. Volume of distribution did not change significantly over the 2 minutes, which implied that vascular volume was filling within the first minute with no subsequent influx into the brain. Previous studies using *in situ* brain perfusion in the rodent have reported brain vascular volumes of 0.007–0.013 ml/g for sucrose (Drion *et al*, 1996 and Dagenais *et al*, 2000) and 0.006–0.009 ml/g for inulin (Takasato *et al*, 1984 and Dagenais *et al*, 2000), another marker of

brain vascular volume. In contrast, these studies adopted an intra-carotid approach and so this value may in fact be an underestimation of the true vascular volume. Data obtained from the application of the transcardiac technique revealed a slightly higher [ $^{14}\text{C}$ ]-sucrose space of  $0.056 \text{ ml/g} \pm 0.008$ , which is equivalent to approximately 5% brain volume. When brain capillaries and all major vessels were combined, the total volume was also  $\sim 5\%$ . Therefore, this value for vascular volume may simply reflect a more complete perfusion of the mouse brain, with no noticeable damage to the BBB.

The *in situ* brain perfusion technique is particularly suitable for assessing transport kinetics by examining transporter saturation (Murakami *et al.*, 2000). To further validate the model, transporter saturation to excitatory amino acids including glutamic acid and glycine were investigated. Glutamic acid does exploit System X<sup>-</sup> on the luminal and the abluminal side of the BBB capillary membrane, whereas glycine is neutral and is transported via the System A carrier which is present at the abluminal membrane and System ASC carrier present at the capillary abluminal membrane in adult animals and also transiently expressed at the luminal membrane in developing animals (Smith *et al.*, 2006). Smith *et al.* (1987) have previously reported values for  $K_m$  and  $V_{max}$  for these amino acids using the brain perfusion technique in rat. However, an extensive literature search did not reveal values for the mouse. These values were estimated, with the transcardiac perfusion, using a kinetic analysis software (GraphPad Prism V 3.02), which calculates transport saturation based on the saturation curve that is generated for each compound. Transport kinetics for glycine were mainly in agreement with the findings of Smith *et al.* (1987). However, glutamic acid displayed  $K_m$  and  $V_{max}$  that were approximately 10 fold greater in the present study. These discrepancies may either reflect differences in transporter affinity and efficacy between species, or between our methodology and that performed by Smith *et al.* (1987).

The *in situ* brain perfusion technique was used also to fix the brain of wild type C57BL/6 mice with lanthanum nitrate in the fixative solution and then the tight junctions were looked more closely using electron microscopy for ultrastructural assessment of blood vessel permeability. Lanthanum nitrate is readily detectable as a black precipitate, which enabled us to distinguish the tracer during the analysis. In this study it was demonstrated that the vessels remain tight during the course of the perfusion. Thus, the integrity of tight junctions remains unaffected in this model.

Once the *in situ* brain perfusion technique was adjusted for optimisation in the mouse and established as a real tool for assessing the penetrance of tracers across the BBB, this method was applied to determine if there were changes to the BBB in Sanfilippo syndrome.

In MPS IIIA mice at 4-6 months of age the brain vascular space assessed with [<sup>14</sup>C]-sucrose resulted significantly reduced compared to controls, and this fact is consistent with the accumulation of GAGs at the endothelial level. In contrast, at 8-10 months this reduction became not significant if assessed with [<sup>14</sup>C]-sucrose while mutant brain vascular volume is still significantly diminished with [<sup>3</sup>H]-inulin as marker.

Cerebral blood flow measured with [<sup>14</sup>C]-diazepam resulted significantly increased at 4-6 months of age in MPS IIIA mice, while this rise became not significant at 8-10 months.

Even when the differences between Sanfilippo A mice and their control strains of mouse were not significant, the spread pattern of perfusions could be considered consistent with the broad continuum of severity in this kind of diseases.

Among carrier-mediated substances with low brain penetrance, it was considered the transport of [<sup>3</sup>H]-glycine, [<sup>3</sup>H]-glutamic acid and [<sup>3</sup>H]-tyrosine. Tyrosine is another neutral amino acid, such as glycine, which uses System L/LAT1 present at both the luminal and abluminal membranes of BBB capillary and System LNAA localized to the abluminal side. In MPS IIIA mice at both 4-6 and 8-10 months of age solely the transport of [<sup>3</sup>H]-glycine resulted significantly increased. One possible explanation could be the fact that carriers for glycine are expressed just in the BBB abluminal capillary membrane, in contrast with carriers for glutamic acid and tyrosine expressed at both the abluminal and luminal sides. Thus the transport of glycine, if somehow unbalanced, may become polarized in the direction of carrier, whilst transports present at both sides of the membrane may cover a possible polarization.

A few preliminary data were obtained also for MPS IIIB mice. Again the significance of the reduction of brain vascular volume assessed with [<sup>14</sup>C]-sucrose at 4-6 months of age in mutant mice compared to controls was not maintained at 8-10 months.

In this model at 8-10 months of age carrier-mediated substance [<sup>3</sup>H]-glutamic acid was not significantly different from the control level, and even [<sup>3</sup>H]-glycine was not increased in a significant way. However, again the spread pattern of perfusions resembles the clinical heterogeneity in Sanfilippo patients.

These initial findings in Sanfilippo syndrome from *in situ* brain perfusion technique, though they need to be confirmed and examined more fully, clearly highlight that some changes occurred in the BBB and point out key molecules, such as sucrose, diazepam and glycine. Since the sucrose data suggests that tight junctions are not compromised, as the vascular space was reduced or comparable to controls and not increased, the significant differences noticed in other tracers may point out modification in the properties of endothelial cell membrane either affecting some transport processes or its permeability.

A further experiment in the understanding of the BBB involved *N*-butyl-deoxynojirimycin (NB-DNJ, miglustat, Zavesca®), one of the small molecules mentioned above that seem to cross the barrier. From perfusion data the unidirectional influx constant of [<sup>3</sup>H]- NB-DNJ into the brain after 1, 2 and 3 minutes was very low, therefore it was decided to conduct intraperitoneal injection with this compound and assess its brain uptake for time intervals of 5, 10, 20, 30, 40, 50 and 60 minutes. This time the unidirectional transfer constant  $K_{in}$  for Zavesca®, though very slow, demonstrated an effective and progressive brain uptake of this small molecule.

In conclusion, in order to improve the knowledge of the BBB, both in health and disease, a very well established experimental tool for assessing the penetrance of tracers across the BBB with great sensitivity was employed, the *in situ* brain perfusion technique. Several aspects of the technique were adjusted for optimisation in the mouse, and the method demonstrated to be successful in perfusing all parts of the mouse brain with a vascular flow that is comparable to literature values (Maeda *et al*, 2000 and Majid *et al*, 2000) and a low enough perfusion pressure not to impair BBB. Indeed, we consider our *in situ* technique to be a greatly improved and robust system for looking into the BBB in mice, and initial important findings were obtained in two mouse models of Sanfilippo syndrome, MPS IIIA and IIIB.

Furthermore, NB-DNJ brain uptake was confirmed by intraperitoneal injection administrations at up to 60 minutes.

Once the extent of BBB involvement and pathology in this mouse models is established, new and improved strategies can be advised to finally repair and cross this barrier in order to treat Sanfilippo syndrome, and neurodegenerative diseases in general, possibly by exploitation of the natural transport pathways.

This study represents a very important tool to understand the mechanisms of the BBB function under physiological conditions as well as during a diseased state. Indeed information obtained will help to develop successful new and improved drugs that may repair the BBB and, in addition, are also capable of crossing the normal BBB without disruption or disturbance of the BBB itself.

## REFERENCES

- Alberts B, Johnson A, Lewis J, Raff M, Roberts K: *Biologia Molecolare della cellula*. Terza edizione. Zanichelli. 1996.
- Aronovich EL, Johnston JM, Wang P, Giger U, Whitley CB. Molecular basis of mucopolysaccharidosis type IIIB in emu (*Dromaius novaehollandiae*): an avian model of Sanfilippo syndrome type B. *Genomics*. 2001 Jun 15;74(3):299-305.
- Banks WA: Physiology and pathology of the blood-brain barrier: implications for microbial pathogenesis, drug delivery and neurodegenerative disorders. *J Neurovirol*. 1999 Dec;5(6):538-55.
- Beart PM, O'Shea RD: Transporters for L-glutamate: an update on their molecular pharmacology and pathological involvement. *Br J Pharmacol*. 2007 Jan;150(1):5-17.
- Beck M: New therapeutic options for lysosomal storage disorders: enzyme replacement, small molecules and gene therapy. *Hum Genet*. 2007 mar;121(1):1-22.
- Begley DJ: Delivery of therapeutic agents to the central nervous system: the problems and the possibilities. *Pharmacol Ther*. 2004 Oct;104(1):29-45.
- Begley DJ: Methods for determining CNS drug transport in animals. In: *Brain barrier systems, Alfred Benzon Symposium 45*. Eds: Paulson O, Knudsen GM, Moos T. Copenhagen: Munksgaard 1999; 91-109.
- Begley DJ: Structure and function of the blood-brain barrier. In: *Enhancement in drug delivery*. Eds: Touitou E, Barry BW. CRC Press, Boca Raton 2007; 575-92.
- Begley DJ: The significance of the blood-brain barrier for Gaucher disease and other lysosomal storage diseases. In: *Gaucher Disease*. Eds: Tony Futerman and Ari Zimran CRC Press and Taylor and Francis. Boca Raton FL. pp 397-421. 2006.
- Begley DJ, Pontikis CC, Scarpa M: Lysosomal storage diseases and the blood-brain barrier. *Curr Pharm Des*. 2008;14(16):1566-80.
- Bhaumik M, Muller VJ, Rozaklis T, Johnson L, Dobrenis K, Bhattacharyya R, Wurzelmann S, Finamore P, Hopwood JJ, Walkley SU, Stanley P: A mouse model for mucopolysaccharidosis type IIIA (Sanfilippo syndrome). *Glycobiology*. 1999 Dec;9(12):1389-96.
- Bickel U, Kang YS, Yoshikawa T, Pardridge WM: *In vivo* demonstration of subcellular localization of antitransferrin receptor monoclonal antibody-colloidal gold conjugate in brain capillary endothelium. *J Histochem Cytochem*. 1994 Nov;42(11):1493-7.

- Blanch L, Weber B, Guo XH, Scott HS, Hopwood JJ: Molecular defects in Sanfilippo syndrome type A. *Hum Molec Genet.* 1997 May;6(5):787-91.
- Chamoles NA, Niizawa G, Blanco M, Gaggioli D, Casentini C: Glycogen storage disease type II: enzymatic screening in dried blood spots on filter paper. *Clin Chim Acta.* 2004 Sep;347(1-2):97-102.
- Constantopoulos G, Dekaban AS: Neurochemistry of the mucopolysaccharidoses: brain lipids and lysosomal enzymes in patients with four types of mucopolysaccharidosis and in normal controls. *J Neurochem.* 1978 May;30(5):965-73.
- Constantopoulos G, Iqbal K, Dekaban AS: Mucopolysaccharidosis type IH, IS, II and IIIA: glycosaminoglycans and lipids of isolated brain cells and other fractions from autopsied tissues. *J Neurochem.* 1980 Jun;34(6):1399-411.
- Dagenais C, Rousselle C, Pollack GM, Scherrmann JM: Development of an in situ mouse brain perfusion model and its application to *mdr1a* P-glycoprotein-deficient mice. *J Cereb Blood Flow Metab.* 2000 Feb;20(2):381-6.
- de Duve C: From Cytases to lysosomes. *Fed Proc.* 1964;23:1045-1049.
- de Duve C: Lysosomes revisited. *Eur J Biochem.* 1983 Dec;137(3):391-7.
- Desnick PW, Schuchman EH: Enzyme replacement and enhancement therapies: lessons from lysosomal disorders. *Nat Rev Genet.* 2002;3(12):954-66.
- Di Natale P, Balzano N, Esposito S, Villani GRD: Identification of Molecular Defects in Italian Sanfilippo A Patients Including 13 Novel Mutations. *Hum Mutat.* 1998; 11(4):313–20.
- Drion N, Lemaire M, Lefauconnier JM, Scherrmann JM: Role of P-glycoprotein in the blood–brain transport of colchicine and vinblastine. *J Neurochem.* 1996 Oct;67(4):1688-93.
- Ellinwood NM, Wang P, Skeen T, Sharp N, Cesta M, Decker S, Edwards NJ, Bublot I, Thompson JN, Bush W, Hardam E, Haskins ME, Giger U: A model of mucopolysaccharidosis IIIB (Sanfilippo syndrome type IIIB): N-acetyl-alpha-D-glucosaminidase deficiency in Schipperke dogs. *J Inherit Metab Dis.* 2003; 26(5):489-504.
- Enns GM, Huhn SM: Central nervous system therapy for lysosomal storage disorders. *Neurosurg Focus.* 2008;24(3-4):E12.
- Eto Y and Ohashi T: Novel treatment for neuronopathic lysosomal storage diseases-cell therapy/gene therapy. *Curr Mol Med.* 2002 Feb; 2(1):83-89.

- Fischer A, Carmichael KP, Munnell JF, Jhabava P, Thompson JN, Matalon R, Jezyk PF, Wang P, Giger U: Sulfamidase deficiency in a family of Dachshunds: a canine model of mucopolysaccharidosis IIIA (Sanfilippo A). *Pediatr Res.* 1998 Jul;44(1):74-82.
- Freeman C, Hopwood JJ: Human liver sulphamate sulphohydrolase. Determinations of native protein and subunit Mr values and influence of substrate agylcone structure on catalytic properties. *Biochem J.* 1986 Feb 15;234(1):83-92.
- Hardebo JE and Nilsson B: Opening of the blood-brain barrier by acute elevation of intracarotid pressure. *Acta Physiol Scand.* 1981 Jan;111(1):43-9.
- Heldermon CD, Hennig AK, Ohlemiller KK, Ogilvie JM, Herzog ED, Breidenbach A, Vogler C, Wozniak DF, Sands MS. Development of sensory, motor and behavioural deficits in the murine model of Sanfilippo syndrome type B. *PLoS ONE.* 2007 Aug 22;2(1):e772.
- Janssen B, Debets J, Leenders P, Smits J: Chronic measurement of cardiac output in conscious mice. *Am J Physiol Regul Integr Comp Physiol.* 2002 Mar;282(3):R928-35.
- Janssen BJ and Smits JF: Autonomic control of blood pressure in mice: basic physiology and effects of genetic modification. *Am J Physiol Regul Integr Comp Physiol.* 2002 Jun. 282(6):R1545-64. Review.
- Jeyakumar M, Dwek RA, Butters TD and Platt FM: Storage solutions: treating lysosomal disorders of the brain. *Nat Rev Neurosci.* 2005 Sep;6(9):713-25.
- Jeyakumar M, Thomas R, Elliot-Smith E, Smith DA, van der Spoel AC, d'Azzo A, Perry VH, Butters TD, Dwek RA, Platt FM: Central nervous system inflammation is a hallmark of pathogenesis in mouse models of GM1 and GM2 gangliosidosis. *Brain.* 2003 Apr;126(Pt 4):974-87.
- Jolly RD, Allan FJ, Collett MG, Rozaklis T, Muller VJ, Hopwood JJ. Mucopolysaccharidosis IIIA (Sanfilippo syndrome) in a New Zealand Huntaway dog with ataxia. *N Z Vet J.* 2000 Oct;48(5):144-8.
- Karageorgos LE, Guo XH, Blanch L, Weber B, Anson DS, Scott HS, Hopwood JJ: Structure and Sequence of the Human Sulphamidase Gene. *DNA Res.* 1996 Aug 31;3(4):269-71.
- LaRue B, Hogg E, Sagare A, Jovanovic S, Maness L, Maurer C, Deane R, Zlokovic BV: Method for measurement of the blood-brain barrier permeability in the perfused mouse brain: application to amyloid-beta peptide in wild type and Alzheimer's Tg2576 mice. *J Neurosci Methods.* 2004 Sep 30;138(1-2):233-42.

- Li HH, Yu WH, Rozengurt N, Zhao HZ, Lyons KM, Anagnostaras S, Fanselow MS, Suzuki K, Vanier MT, Neufeld EF. Mouse model of Sanfilippo syndrome type B produced by targeted disruption of the gene encoding alpha-N-acetylglucosaminidase. *Proc Natl Acad Sci U S A*. 1999 Dec 7;96(25):14505-10.
- Li HH, Zhao HZ, Neufeld EF, Cai Y, Gómez-Pinilla F: *J Neurosci Res*. 2002 Jul 1;69(1):30-8.
- Lim MJ, Alexander N, Benedict JW, Chattopadhyay S, Shemilt SJ, Guérin CJ, Cooper JD, Pearce DA: IgG entry and deposition are components of the neuroimmune response in Batten disease. *Neurobiol Dis*. 2007 Feb;25(2):239-51.
- Lodish H, Baltimore D, Berk A, Matsudaira P, Kaiser CA, Krieger M, Scott MP, Zipursky L, Darnell J: *Molecular Cell Biology*. Scientific American Books. 2002.
- Maeda K, Mies G, Olah L, Hossmann KA: Quantitative measurement of local cerebral blood flow in the anesthetized mouse using intraperitoneal [<sup>14</sup>C]iodoantipyrine injection and final arterial heart blood sampling. *JCBFM* 2000 Jan;20(1):10-14.
- Majid A, He YY, Gidday JM, Kaplan SS, Gonzales ER, Park TS, Fenstermacher JD, Wei L, Choi DW, Hsu CY: Differences in vulnerability to permanent focal cerebral ischemia among 3 common mouse strains. *Stroke* 2000 Nov ;31(11): 2707-2714.
- Meikle PJ, Hopwood JJ, Clague AE, Carey WF: Prevalence of lysosomal storage disorders. *JAMA*. 1999 Jan 20;281(3):249-54.
- Meikle PJ, Ranieri E, Simonsen H, Rozaklis T, Ramsay SL, Whitfield PD, Fuller M, Christensen E, Skovby F, Hopwood JJ: Newborn screening for lysosomal storage disorders: clinical evaluation of a two-tier strategy. *Pediatrics*. 2004 Oct;114(4):909-16.
- Muenzer J: The mucopolysaccharidoses: a heterogeneous group of disorders with variable pediatric presentations. *J Pediatr*. 2004 May;144(5 Suppl):S27-S34.
- Murakami H, Takanaga H, Matsuo H, Ohtani H, Sawada Y: Comparison of blood-brain barrier permeability in mice and rats using in situ brain perfusion technique. *Am J Physiol Heart Circ Physiol*. 2000 Sep;279(3):1022-8.
- Nag S. and Begley DJ: Blood-brain barrier, exchange of metabolites and gases. In: *Cerebrovascular Diseases*. Kalimo H. Ed. ISN Neuropath Press, Basel. pp 22-29, 2005.
- Neufeld EF and Muenzer J: The mucopolysaccharidoses. In: *The metabolic and molecular bases of inherited disease*. Eds: Scriver CR, Beaudet AL, Sly WS, Valle D. McGraw-Hill, New York. pp 2465-2494, 1995.
- Neufeld EF and Muenzer J: The mucopolysaccharidoses. In: *The Metabolic and Molecular Basis of Inherited Disease*, 8 ed, Vol III. Eds: Scriver CR, Beaudet AL, Sly

WS, Valle D, Childs B, Kinzler KW, Vogelstein B. McGraw-Hill, Medical Publishing Division, p 3421. 2001.

- Ohmi K, Greenberg DS, Rajavel KS, Ryazantsev S, Li HH and Neufeld EF: Activated microglia in cortex of mouse models of mucopolysaccharidoses I and IIIB. Proc Natl Acad Sci. USA 2003 Feb;100(4):1902-7.
- Platt FM, Walkley SU: Lysosomal Disorders of the Brain. Oxford University Press. 2004.
- Rapoport SI: Opening of the blood-brain barrier by acute hypertension. Exp Neurol. 1976 Sep;52(3):467-79.
- Schwarze SR, Ho A, Vocero-Akbani A, Dowdy SF: *In vivo* protein transduction: delivery of a biologically active protein into the mouse. Science. 1999 Sep 3;285(5433):1569-72.
- Scott HS, Blanch L, Guo XH, Freeman C, Orsborn A, Baker E, Sutherland GR, Morris CP, Hopwood JJ: Cloning of the sulphamidase gene and identification of mutations in Sanfilippo A syndrome. Nat Genet. 1995 Dec;11(4):465-7.
- Smith QR, Momma S, Aoyagi M, Rapoport SI. Kinetics of neutral amino acid transport across the blood-brain barrier. J Neurochem. 1987 Nov;49(5):1651-8.
- Smith QR, Mandula H, Parepally JMR: Amino acid transport across the blood-brain barrier. Chapter 197. In: Handbook of biologically Active Peptides. Ed: Kasta AJ. Academic Press, pp1415-1422. 2006.
- Takasato Y, Rapoport SI, Smith QR: An in situ brain perfusion technique to study cerebrovascular transport in the rat. Am J Physiol 1984 Sep;247(3 Pt 2): H484-H493.
- Triguero D, Buciak J, Pardridge WM: Capillary depletion method for quantification of blood-brain barrier transport of circulating peptides and plasma proteins. J Neurochem. 1990 Jun;54(6):1882-8.
- Urayama A, Grubb JH, Sly WS, Banks WA: Developmentally regulated mannose 6-phosphate receptor-mediated transport of a lysosomal enzyme across the blood-brain barrier. Proc Natl Acad Sci. USA 2004 Aug 24;101(34):12658-63.
- von Figura K, Hasilik A, Steckel F, Van De Kamp J: Biosynthesis and Maturation of a-N-Acetylglucosaminidase in Normal and Sanfilippo B-Fibroblasts. Am J Hum Genet. 1984 Jan;36(1):93-100.
- Wada R, Tiffit CJ and Proia RL: Microglial activation precedes acute neurodegeneration in Sandhoff disease and is suppressed by bone marrow transplantation. Proc Natl Acad Sci. USA 2000 Sep;97(20):10954-9.

- Ward R, Collins RL, Tanguay G, Miceli D: A quantitative study of cerebrovascular variation in inbred mice. *J Anat* 1990 Dec;173: 87-95.
- Weber B, Blanch L, Clements PR, Scott HS, Hopwood JJ: Cloning and expression of the gene involved in Sanfilippo B syndrome (mucopolysaccharidosis III B). *Hum Mol Genet.* 1996 Jun;5(6):771-7.
- Weber B, Guo HX, Wraith JE, Cooper A, Kleijer WJ, Bunge S, Hopwood JJ: Novel mutations in Sanfilippo A syndrome: implications for enzyme function. *Hum Mol Genet.* 1997 Sep;6(9):1573-9.
- Wenk J, Hille A, von Figura K: Quantitation of Mr 46000 and Mr 30000 mannose 6-phosphate receptors in human cells and tissues. *Biochem Int.* 1991 Mar;23(4):723-31.
- Winchester B, Vellodi A, Young E: The molecular basis of lysosomal storage diseases and their treatment. *Biochem Soc Trans.* 2000 Feb;28(2):150-4.
- Yogalingam G, Weber B, Meehan J, Rogers J, Hopwood JJ: Mucopolysaccharidosis type IIIB: characterisation and expression of wild-type and mutant recombinant alpha-N-acetylglucosaminidase and relationship with Sanfilippo phenotype in an attenuated patient. *Biochim Biophys Acta.* 2000 Nov 15;1502(3): 415-25.
- Zhang Y, Pardridge WM: Delivery of beta-galactosidase to mouse brain via the blood-brain barrier transferrin receptor. *J Pharmacol Exp Ther.* 2005 Jun;313(3):1075-81.
- Zhao HG, Li HH, Bach G, Schmidtchen A, Neufeld EF: The molecular basis of Sanfilippo syndrome type B. *Proc Natl Acad Sci. USA* 1996 June 11;93(12):6101-5.
- Zloković BV, Begley DJ, Djurčić BM, Mitrović DM: Measurement of solute transport across the blood-brain barrier in the perfused guinea pig brain: method and application to N-methyl-alpha-aminoisobutyric acid. *J Neurochem.* 1986 May;46(5):1444-51.



